

Opening and Closing DNA: Theories on the Nucleosome

IGOR M. KULIĆ and HELMUT SCHIESSEL

7.1 INTRODUCTION

DNA—the carrier of the genetic information—is at the base of many central life processes [1]: replication, transcription, and repair of genetic material depend on the unique properties of DNA, especially the base pairing. One has, however, to appreciate the fact that the molecular machinery of eucaryotes (plants and animals) does not deal with naked DNA but with chromatin, a DNA–protein complex in which DNA is wrapped and folded in a hierarchical fashion [2]. On the lowest level DNA is wrapped nearly twice around an octamer of histone proteins. A short stretch of the “linker DNA” connects to the next such protein spool. The resulting string of so-called nucleosomes folds into higher order structures, the details of which are still under debate (see Figure 7.1).

The structure of the nucleosome core particle (NCP), the particle that is left when the linker DNA is digested away, is known in exquisite detail from X-ray crystallography at 2.8 Å resolution [3] and more recently at 1.9 Å [4]. The octamer is composed of two molecules each of the four core histone proteins H2A, H2B, H3, and H4. At physiological conditions the stable oligomeric aggregates of the core histones are the H3–H4 tetramer (an aggregate of two H3 and two H4 proteins) and the H2A–H2B dimer; the octamer is then only stable if it is associated with DNA [5]. The two dimers and the tetramer are put together in such a way that the resulting octamer forms a cylinder with about a 65 Å diameter and about a 60 Å height. With grooves, ridges, and binding sites the octamer defines the wrapping path of the DNA, a left-handed helical ramp of 1 and 3/4 turns, a 147 base-pairs (bp) length, and a roughly 28 Å pitch. This aggregate has a twofold axis of symmetry (the dyad axis) that is perpendicular to the superhelix axis. A schematic view of the NCP is given in Figure 7.2.

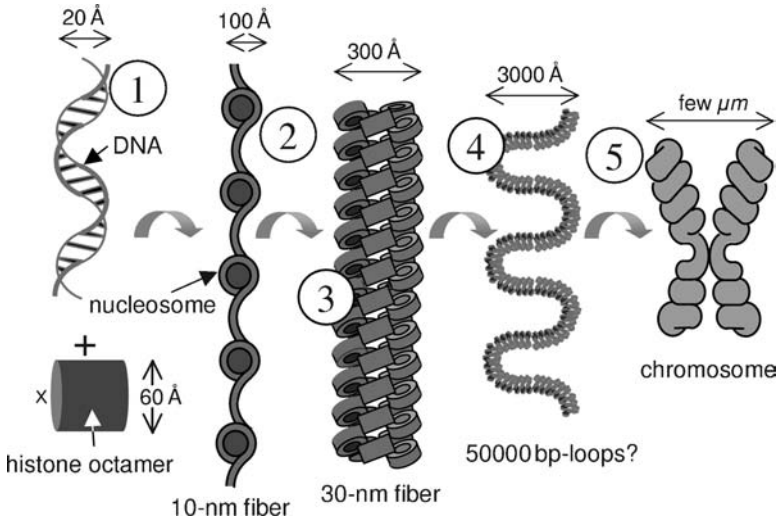


Figure 7.1 Steps of DNA compaction: (1) DNA, (2) nucleosomes, (3) chromatin fiber, (4) higher order structures, and (5) the mitotic chromosome. Details of the structures beyond the nucleosome are still under debate. (See color plate.)

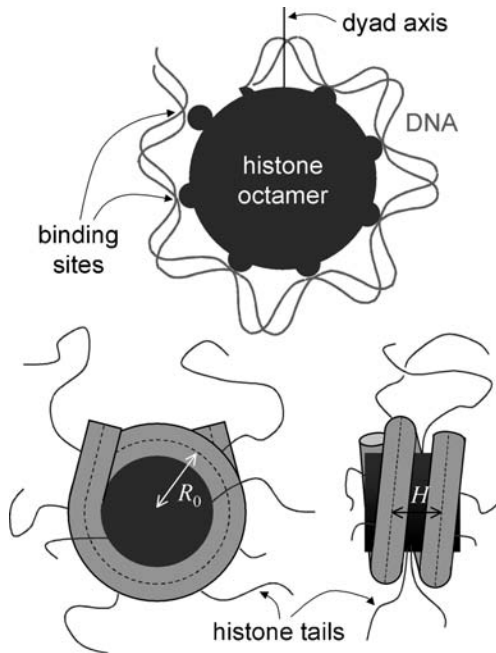


Figure 7.2 Schematic views of the NCP. The top image shows only the upper half of the wrapped DNA with its binding points to the histone octamer located at the positions where the minor groove faces the cylinder. At the bottom the full NCP is shown from the top and from the side including the eight histone tails.

There are 14 regions where the wrapped DNA contacts the octamer surface, as documented in detail in [4]. These regions are located where the minor grooves of the right-handed DNA double helix face inward toward the surface of the octamer. At each contact region there are several direct hydrogen bonds between the histone proteins and the DNA sugar-phosphate backbone [3] as well as bridging water molecules [4]. In addition there is always a (cationic) arginine side chain extending into the DNA minor groove. However, no reliable quantitative estimate of the free energy of binding per sticking point has yet been made.

An indirect method used to estimate these values is based on studies of competitive protein binding to nucleosomal DNA [6,7], as we will discuss in more detail in Section 7.2. From these experiments it can be estimated that the adsorption energy per sticking point is roughly of the order $1.5 - 2k_B T$, a number that—as we will show in the next section—has to be taken with caution. If we believe in this number for the moment, we should do so with awareness of the fact that the $1.5 - 2k_B T$ does not represent the *pure* adsorption energy but instead the *net* gain in energy that is left after the DNA has bent around the octamer to make contact with the sticking point. A rough estimate of the deformation energy can be obtained by describing the DNA as a semiflexible chain with a persistence length l_p of about 500 \AA [8]. Then the elastic energy [9] required to bend the 127 bp of DNA around the octamer (10 bp at each terminus are essentially straight [3]) is given by

$$\frac{E_{elastic}}{k_B T} = \frac{l_p l}{2R_0^2}. \quad (7.1)$$

Here l is the bent part of the wrapped DNA, roughly $127 \times 3.4 \text{ \AA} = 432 \text{ \AA}$, and R_0 is the radius of curvature of the centerline of the wrapped DNA (see Figure 7.2) that is about 43 \AA [3]. As a result the bending energy is of order $58k_B T$, a number, however, that has again to be taken with caution because it is not clear that equation (7.1) can hold up to such strong curvature. In particular, DNA does not bend uniformly around the octamer [10,11]. But in using these numbers, we can estimate the bending energy per 10 base pairs (i.e., per sticking site) to be of the order $60k_B T / 14 \approx 4k_B T$ [5].

Together with the observation that the net gain per sticking point is around $2k_B T$, this means that the pure adsorption energy is on average roughly $6k_B T$ per binding site. Note that a huge pure adsorption energy of $6k_B T \times 14 \approx 85k_B T$ per nucleosome is canceled to a large extent by $58k_B T$ from the DNA bending, a fact that has important consequences for nucleosomal dynamics.

Of great importance are also the flexible, irregular tail regions of the core histones that make up roughly 28% of their sequences [12]. Each histone protein has a highly positively charged, flexible tail (the N-end of the polypeptide chain) that extends out of the nucleosome structure. Some tails exit between the two turns of the wrapped DNA, and others on the top or bottom of the octameric cylinder. These N-tails are extremely basic due to a high amount of lysine and arginine residues. They are sites of posttranslational modifications and are crucial for chromatin regulation. The tails have an especially strong influence on the higher order structure of chromatin.

In this chapter we describe several mechanisms that are of importance for releasing the DNA wrapped into nucleosomes. In the next section, we discuss forced nucleosome unwrapping and spontaneous “site exposure.” In Section 7.3 we focus on nucleosome sliding along DNA, which is also of importance for the interaction between nucleosomes and RNA polymerase, the subject of Section 7.4. Section 7.5 is devoted to the tail-bridging mechanism that causes attraction between nucleosomes. In the last section, we provide some conclusions.

7.2 UNWRAPPING NUCLEOSOMES

Consider a DNA fragment containing one nucleosome under an external force applied at the DNA termini. Clearly, for large enough forces, the DNA unwraps from the octamer and the nucleosome falls apart. What is the critical force that is necessary to induce such an unwrapping? The answer seems to be straightforward: the length that is stored in the nucleosome is 147 bp—that is, 50 nm—and the net adsorption energy of these 50 nm amounts to roughly $30k_B T$. Unwrapping the nucleosome means to release this wrapped length by paying the price of the net adsorption energy. Beyond a critical force unwrapping is favorable, with the critical force being given by

$$F_{crit} \approx \frac{30k_B T}{50 \text{ nm}} = 2.5 \text{ pN}. \quad (7.2)$$

The same critical force should be expected if there are several nucleosomes associated with the DNA fragment; all the nucleosomes should unwrap in parallel at the same critical force. As it turns out this line of reasoning is much too simple to capture the physics of the unwrapping process. Moreover the numbers involved in (7.2) are probably far off the real values.

A recently performed experiment [13] on a fiber of nucleosomes assembled from purified histones via salt dialysis made observations that are indeed very different from what (7.2) predicts (see also the related experiments on native and reconstituted chromatin fibers [14–17]). The experiment was performed with a DNA chain with up to 17 nucleosomes complexed at well-defined positions (the DNA featuring tandemly repeated nucleosome positioning sequences, base-pair sequences that have a higher affinity to histone octamers than average DNA; see Section 7.3 for more details). When small forces ($F < 10$ pN) were applied for short times (≈ 1 – 10 s), the nucleosome unwrapped only partially by releasing the outer 60 to 70 bp of wrapped DNA in a gradual and equilibrium fashion. For higher forces ($F > 20$ pN), the nucleosomes showed a pronounced sudden nonequilibrium release behavior of the remaining 80 bp, with the latter force being much larger than that expected by the equilibrium argument above. To explain this peculiar finding, Brower-Toland et al. [13] conjectured that there must be a barrier of around $38k_B T$ in the adsorption energy located after the first 70 to 80 bp and smeared out over not more than 10 bp, so as to reflect some biochemical specificity of the nucleosome structure at that position. However, there is no experimental indication of such a huge specific barrier, not from the crystal structure

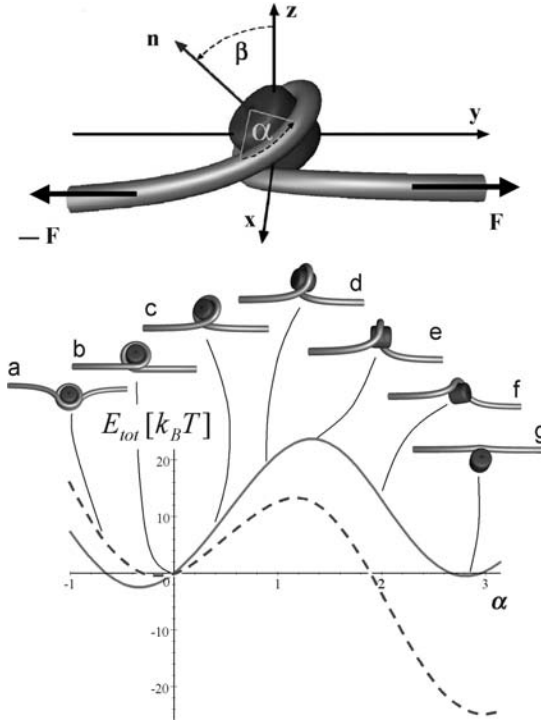


Figure 7.3 The nucleosome under tension. The top image shows the two angles involved in the unwrapping process: the desorption angle α and the tilting angle β . The bottom shows the nucleosome unwrapping that involves a 180° rotation of the octamer and the associated energy, equation (7.6), as a function of α for an applied tension of 6.5 pN. The dashed curve represents a typical “traditional” estimate of adsorption energy density, $k^a = 2k_B T/\text{nm}$, where the applied force is far beyond the critical force. For the solid curve we choose $k^a = 3k_B T/\text{nm}$ to account for the first-second round difference (18) where the applied tension of 6.5 pN corresponds to the critical force. Note that in both cases unwrapping is only possible as an activated process going across a substantial barrier.

[4] nor from the equilibrium accessibility to nucleosomal DNA [6]. In [18] we have argued that the barrier is caused by the underlying geometry and physics of the DNA spool rather than by a specific biochemistry of the nucleosome.

Our model [18] of a DNA spool under tension is shown in the upper half of Figure 7.3. The DNA is represented by a worm-like chain (WLC) which provides a good description of the mechanical properties of the DNA [19]. The WLC is a semiflexible tube characterized by two moduli, the bending and the torsional stiffnesses. The torsional stiffness is neglected, since in the experiment the ends are freely rotating [13]. The elastic energy of a WLC of length L can then be expressed as

$$E_{bend} = \frac{A}{2} \int_0^L ds \kappa^2(s). \quad (7.3)$$

Here A is the bending stiffness and $\kappa(s)$ the curvature of the chain at point s along its contour. The stiffness is related to the orientational persistence length l_p via $A = k_B T l_p$; in fact (7.1) is a special case of (7.3). The DNA is assumed to be adsorbed on the protein spool surface along the predefined helical path with radius R_0 and pitch height H : see the lower image of Figure 7.2, with a pure adsorption energy density per wrapped length, k^a , given by the pure attraction of the binding sites (not including the bending contribution).

The degree of DNA adsorption is described by the desorption angle α , which is defined to be zero for one full turn wrapped (see the top image of Figure 7.3). It is immediately clear that the unwrapping problem is nonplanar and that the spool needs to rotate transiently out of the plane while performing a full turn—an effect already pointed out by Cui and Bustamante [14]. Therefore a second angle, β , is introduced to describe the out-of-plane tilting of the spool as shown in Figure 7.3. When a tension F along the Y -axis acts on the two outgoing DNA “arms,” the system (i.e., the wrapped spool together with the free DNA ends) will simultaneously respond with DNA deformation, spool tilting, and DNA desorption from the spool.

The total energy of the system as a function of α and β has three contributions:

$$E_{tot}(\alpha, \beta) = E_{bend} + 2R_0 k^a \alpha - 2F \Delta y. \quad (7.4)$$

The first term in (7.4) is the deformation energy of the DNA chain, equation (7.3), the second describes the desorption cost, and the third term represents the potential energy gained by pulling out the DNA ends, each by a distance Δy .

It is possible to work out analytically the total energy by calculating the shape and energy of the DNA arms accounting for the right boundary conditions at the points where the DNA enters and leaves the spool and at the DNA termini (which are assumed to be far from the spool). Instead of giving the full analytical expression of E_{tot} (provided in [18]), we only present here the limit for a flat spool with $R_0 \gg H$. In this case

$$E_{tot}(\alpha, \beta) = 2R_0 \left[k^a - \frac{A}{2R_0^2} - F \right] \alpha + 2FR_0 \cos \beta \sin \alpha + 8\sqrt{AF} \left[1 - \sqrt{\frac{1 + \cos \alpha \cos \beta}{2}} \right]. \quad (7.5)$$

This is a reasonably good approximation for the nucleosome where $R_0 = 43$ nm is larger than $H = 2.4$ nm. In (7.5) the first term describes the competition between adsorption favoring the formation of the spool and the bending and external tension, both favoring the unwrapping of the DNA. The second term is a geometrical term that describes gain and loss of potential energy due to spool unwrapping (change in α) and rotation (change in β). The last and most important term accounts for bending energy of the arms and the cost of potential energy because of the arms not being straight.

The energy landscape is mainly governed by that last term in (7.5). If we neglect the geometrical term (which one can easily check is a reasonable approximation) and go to the critical force at which the first term on the rhs of (7.5) vanishes, $F_{crit} = k^a - A/(2R_0^2)$, then the transition path of the nucleosome is going along the line $\alpha = \beta$ from the minimum at $(\alpha, \beta) = (0, 0)$ over the saddle point $(\pi/2, \pi/2)$ to another minimum of the same height at (π, π) . The barrier height is given by $\Delta U \approx \Delta E_{tot} = 8\sqrt{AF}(1 - 1/\sqrt{2})$, and it mainly stems from the strong bending of the DNA arms in the transition state; see configuration e in Figure 7.3.

As this suggests, a reasonable approximation is to set $\alpha = \beta$ in the full energy expression, (7.5):

$$E_{tot}(\alpha) \approx 2R_0 \left[k^a - \frac{A}{2R_0^2} - F \right] \alpha + 2FR_0 \cos \alpha \sin \alpha + 8\sqrt{AF} \left[1 - \sqrt{\frac{1 + \cos^2 \alpha}{2}} \right]. \quad (7.6)$$

In Figure 7.3 we plot the resulting energy landscape for a force of $F = 6.5$ pN. The dashed curve corresponds to the value $k^a = 2k_B T/\text{nm}$ as inferred from competitive protein binding data (see Section 7.1); for the solid curve we assume a larger value, $k^a = 3k_B T/\text{nm}$ (see below).

To compare our model to the unwrapping experiment [13], we need to account for the fact that it was performed using dynamical force spectroscopy (DFS) [20]. The nucleosomal array was exposed to a force F increasing at constant rate r_F , $F = r_F t$; the probable rupture force F^* as a function of loading rate was determined in a series of measurements. The rate of unwrapping is expected to be proportional to the Kramers's rate [21] $\exp(\Delta U - \pi R_0(F_{crit} - F))$ from which it can be shown that $F^* \propto \ln(r_F) + \text{const}$.

To our surprise, our detailed analysis [18] showed that the rates over the barrier are much too fast in our model as compared to the rates at which nucleosomes unwrap in the experiment. This forced us to critically reconsider the assumptions on which the model was based, especially the seemingly straightforward assumption that the adsorption energy per length is constant along the wrapping path. By this assumption, we neglected an important feature of the nucleosome, namely that the two DNA turns interact. Clearly, the turns are close enough to feel a considerable electrostatic repulsion, the exact amount of which is hard to be determined, such as that due to the fact that the DNA is adsorbed on the low-dielectric protein core (image effects). Moreover the presence of histone tails complicates things. It is known (see Section 7.5) that the tails adsorb on the nucleosomal DNA. If the nucleosome is fully wrapped, the two turns have to share the cationic tails. However, if there is only one turn left, all these tails can, in principle, adsorb on this remaining turn. All these effects go in one direction: a remaining DNA turn on the wrapped nucleosome is much stronger adsorbed than a turn in the presence of the second, wrapped turn. Indeed very recent data by the same experimental group show that the force peaks of the discontinuous unwrapping events shift to substantially smaller values when the tail are partly removed or their charges partially neutralized [22].



Figure 7.4 The site exposure mechanism [6,7] allows access to wrapped DNA via the spontaneous unraveling of DNA. When only one turn is left (shown in dark gray), that remaining turn results in a strong grip on the octamer, and further unpeeling becomes too costly (first-second round difference [18]).

The crucial point is now that the adsorption energy k^a was estimated from spontaneous unwrapping events of the second turn in the presence of the other turn [6,7] and thus k^a might have been strongly underestimated, since the $k^a = 2.0k_B T/\text{nm}$ include the unfavorable repulsion from the other turn. To account for this we assumed that there is a different effective value of k^a for $\alpha > 0$ (less than one DNA turn) and for $\alpha < 0$ (more than one turn) [18]. Because the discontinuous unwrapping events observed in the experiment clearly corresponded to the case where the last term is unwrapped (i.e., to the case $\alpha > 0$), we tuned the parameter k^a such that we could reproduce the DFS data in a satisfying way. From this we found that for $\alpha > 0$ a value of $k^a = 3.0 - 3.5k_B T/\text{nm}$ leads to good agreement with the experimental data, a value that is *considerably* higher than the effective adsorption energy $k^a = 2k_B T/\text{nm}$ felt when a turn is unpeeled in the presence of the other turn, meaning for $\alpha < 0$.

This result might explain how wrapped DNA inside a nucleosome is accessible to DNA binding proteins while the nucleosome remains stable. As long as the nucleosome is fully wrapped, many DNA binding proteins have no access to the wrapped DNA portion (reviewed in [23]). But it is also in this fully wrapped conformation that each of two turns can easily unwrap spontaneously because of thermal fluctuations. Therefore all DNA is transiently accessible for DNA binding proteins, as depicted in Figure 7.4. This fact has been proved experimentally via competitive protein binding by Widom and coworkers, and it has been termed the site exposure mechanism [6,7]. Recently fluorescence resonance energy transfer measurements have provided additional and more direct evidence for such conformational fluctuations [24,25]. What is nevertheless puzzling in this set of experiments is why the DNA—once it encounters the nucleosomal dyad—stops unpeeling, which then leads to the destruction of the nucleosome. Our interpretation of the unwrapping data suggests that the reason for this is the first-second round difference: once the DNA has unpeeled one turn, the remaining turn has a strong grip on the octamer because this turn does not feel the repulsion from the other turn.

7.3 NUCLEOSOME SLIDING

It has been observed under well-defined in vitro conditions that nucleosomes spontaneously reposition along DNA [26–29] transforming nucleosomal DNA into

free DNA, and vice versa, a phenomenon referred to as nucleosome “sliding.” This heat-induced repositioning is a rather slow process happening on the time scale of minutes to hours. This suggests that *in vivo* octamer repositioning must be catalysed. Indeed ATP-consuming machines, so-called chromatin remodeling complexes, are known that actively push or pull nucleosomes along DNA [30,31].

Repositioning experiments (a detailed review is provided in [5]) have mostly been performed on short DNA fragments of lengths around 200 to 400 bp that contain one or two so-called positioning sequences. Repositioning is detected with the help of 2D gel electrophoresis making use of the fact that a complex with its octamer close to one of the DNA termini shows a higher electrophoretic mobility [26–28] than a complex where the octamer is located at the center of the DNA fragment. Another approach [29] makes use of a chemically modified histone protein that induces a cut on the nucleosomal DNA. What came out of these studies is that heat-induced repositioning is a slow process that takes place on the time scale of minutes to hours [26,29] at elevated temperatures (e.g., 37°C), whereas it is not observed at low temperatures (e.g., 5°C). Another interesting feature is that the octamer is found at a preferred position (as was mentioned above, the DNA contains a positioning sequence) or shifted in multiples of 10 bp, the DNA helical pitch, away from this position [26,29]; in addition there is a preference for end positions [26]. On longer DNA fragments no evidence for a long-range repositioning has been found [27]. And finally, the presence of linker histones (H1 or H5) suppresses nucleosome mobility [28].

What causes nucleosome mobility? It is obvious that an ordinary sliding of the DNA on the protein spool is energetically too costly. As was mentioned above, the interaction between the DNA and the octamer is localized at 14 binding sites, each contributing roughly $6k_B T$ pure adsorption energy. A bulk sliding motion would involve the simultaneous breakage of these 14 point contacts, an event that would never occur spontaneously. As an alternative mechanism, a rolling motion of the octamer along the DNA makes also no sense: the helical wrapping path would simply cause the cylinder to roll off the DNA.

Repositioning must thus involve intermediates with a lower energetic penalty. The two possible mechanisms [5,32] are based on small defects that spontaneously form in the wrapped DNA portion and propagate through the nucleosome: 10 bp bulges [33,34] (see Figure 7.5*a*) and 1 bp twist defects [35] (see Figure 7.5*b*). The basic idea of the bulge mechanism is as follows: First some DNA unpeels spontaneously from one of the termini of the wrapped portion [6,7]. Then that DNA is pulled in before it re-adsorbs, creating an intranucleosomal DNA bulge that stores some extra length ΔL . This bulge diffuses along the wrapped DNA portion and finally leaves the nucleosome at either end. If the loop comes out at the end where it was formed, the DNA is back at the original state. But if the loop leaves at the other end, the stored length ΔL has effectively been transported through the nucleosome and the octamer has moved by ΔL along the DNA. A careful quantitative analysis provided in [34] shows that the cheapest small loop has a length of $\Delta L = 10$ bp. Other loops are by far more expensive because they require twisting and/or stronger bending. But even a 10 bp loop is very expensive, since its formation requires about $20k_B T$ desorption and bending energy. As a consequence the corresponding diffusion

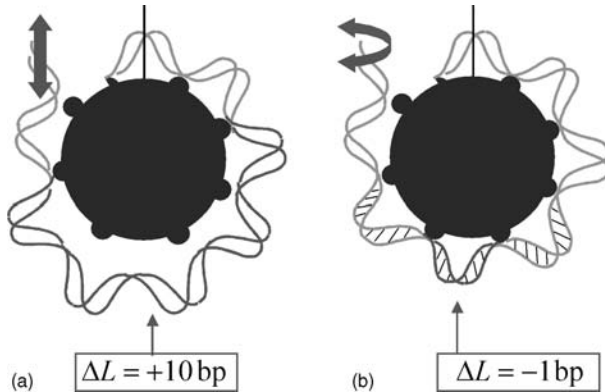


Figure 7.5 Two possible mechanisms underlying the spontaneous repositioning of nucleosomes: Formation of (a) bulge defects and (b) twist defects. Bulge defects contain typically an excess length of 10 bp, leading to repositioning steps of 10 bp that in turn preserve the rotational positioning of the nucleosome. Twist defects carry either an extra or a missing base pair. This results in 1 bp repositioning steps and a concomitant corkscrew motion of the nucleosome.

constant of the octamer along the DNA was found to be very small, namely on the order of $D \approx 10 - 16 \text{ cm}^2/\text{s}$. Thus typical repositioning times on a 200 bp DNA fragment are on the order of an hour, in reasonable agreement with the experimental data [26,29]. The strong temperature dependence and most strikingly the preference for 10 bp steps—corresponding to the extra length stored in the cheapest loops—is also in excellent agreement with the experiments. All these facts strongly support the idea that the loops are the mechanism underlying repositioning. There is, however, one serious caveat: we found that larger loops beyond one persistence length of DNA (roughly 150 bp) are easier to form than 10 bp bulges, since such loops show a small curvature and have less desorbed binding sites [34]. Of course, for short DNA segments such loops cannot occur. But even in experiments with DNA segments of roughly 400 bp length, no signature of a long-range nucleosome repositioning has been found [27].

This observation led us to reconsider the underlying mechanism and to check whether nucleosome repositioning could be based on twist defects instead [35]. The basic idea is here that a twist defect forms spontaneously at either end of the wrapped DNA portion. Such a defect carries either a missing or an extra bp (Figure 7.5b shows a missing bp). A defect is typically localized between two neighboring nucleosomal binding sites, meaning within one helical pitch (10 bp). This short DNA portion is stretched (compressed) and overtwisted (undertwisted). The energy of a ± 1 bp twist defects was estimated from the combined stretch and twist elasticity of DNA, including the (here unfavorable) twist–stretch coupling to be on the order of $9k_B T$ [35]. That means that, at a given time, a twist defect occurs only on one of around thousand nucleosomes.

Once a twist defect has formed, it diffuses through the wrapped DNA portion. The nucleosome provides between its 14 binding sites 13 positions for the defect. A defect, say a “hole” with a missing bp, moves from one position to the next in the fashion of an earthworm creep motion. The bp that is in contact with a binding site moves toward the defect, resulting in an intermediate state where the defect is stretched out over 20 bp, which lowers the elastic strain but costs desorption energy. Once the next bp has bound to the nucleosome, the twist defect has moved to the neighboring location. During this process the kink has to cross an energetic barrier on the order of $2k_B T$ [35]. Of course, not all twist defects that have formed will reach the other end of the nucleosome; most fall off at the end at which they have been created. By assuming that all 13 possible defect locations are energetically equivalent, we can show that only 1/13 of the defects reach ultimately the other end and causes the nucleosomal mobility. Once such a twist defect has been released at the other end, the octamer makes a step by one bp *and* a rotation by 36° around the DNA axis. This motion can also be interpreted as a corkscrew motion of the DNA on the nucleosome.

Twist defects lead to shorter step sizes of the octamer as compared to loop defects (1 bp vs. 10 bp), but this shorter length is dramatically overcompensated by their lower activation cost (roughly $9k_B T$ vs. $20k_B T$). In fact, by putting all the points given above together, we were able to estimate the diffusion constant of the nucleosome along DNA to be $D_0 \approx 580 \text{ bp}^2/\text{s} \approx 7 \times 10^{-13} \text{ cm}^2/\text{s}$ that is three to four orders of magnitude larger than the one predicted by the loop defects [35].

The typical repositioning times on a 200 bp piece of DNA are thus predicted to be on the order of a second, a time much shorter than in the experiments. Also the predicted dependence of the dynamics on temperature is much too weak. Even worse, there is no “built-in” mechanism for 10 bp steps of the octamer. The experimentally observed preference for positions 10 bp apart manifesting itself in characteristic bands in the products of the gel electrophoresis [26,27] seems to be inconsistent with this mechanism—at least at first sight.

Here comes into a play an important additional feature of the repositioning experiments: that they are typically performed with DNA segments containing strong positioning sequences, especially the sea urchin 5S positioning element [26–28]. This sequence shows a highly anisotropic bendability of the DNA. If repositioning is based on twist defect, then the DNA has to bend in the course of a 10 bp shift in all directions, and thus has to go over a barrier. The elastic energy of the bent DNA is then a periodic function of the nucleosome position with the helical pitch constituting the period. We approximated this energy by an idealized potential of the form $U(l) = (A/2)\cos(2\pi l/10)$, with l being the bp number and A denoting the difference in elastic energy between the optimal and the worst rotational setting [34]. In principle, these oscillations die out completely when the nucleosome leaves the positioning sequence, that is, if it has moved around 140 bp. But since the templates are usually quite short (e.g., 216 bp [36]), the nucleosome always feels the rotational signal from the positioning sequence and our elastic energy should provide a reasonable description. As a result the nucleosomal diffusion constant is

reduced to the value [35]:

$$D = \frac{D_0}{I_0^2(A/2k_B T)} \cong \begin{cases} \frac{D_0}{1+A^2/8(k_B T)^2} & \text{for } A < k_B T, \\ D_0 \frac{\pi A}{k_B T} e^{-A/k_B T} & \text{for } A \gg k_B T, \end{cases} \quad (7.7)$$

where I_0 denotes the modified Bessel function. D_0 is the diffusion constant for homogeneously bendable DNA that we estimated above to be on the order of $580 \text{ bp}^2/\text{s}$.

For the sea urchin 5S positioning element, $A \approx 9k_B T$ [37,38] leads to a reduced mobility with $D \approx 2 \times 10^{-15} \text{ cm}^2/\text{s}$. The typical repositioning times on a 200 bp DNA segment are now two to three orders of magnitude longer, meaning, they are on the order of an hour—remarkably just as the ones predicted for the loop case. It is now a simple matter of equilibrium thermodynamics that the probability of finding the DNA wrapped in its preferred bending direction is much higher than in an unfavorable direction. Thus also in the case of 1 bp defects we expect to find nucleosomes mostly at the optimal position or 10, 20, 30, and so forth, bp apart corresponding to locations where still most of the positioning sequence is associated with the octamer and this in the preferred rotational setting. The bands in the gel electrophoresis experiments have then to be interpreted as a reflection of the Boltzmann distribution of the nucleosome positions rather than of the intrinsic step length. In other words, both the 10 bp bulge and the 1 bp twist defect lead in the presence of a rotational positioning sequences to pretty much the same prediction for the experimentally observed repositioning—even though the elementary motion is fundamentally different.

We come now to the question whether there are experimental data available from which the underlying mechanism can be induced. The most straightforward test would be to use a DNA template with less exotic mechanical properties. On an isotropically bendable DNA template, a nucleosome's mobility should not be affected if it relies on the loop mechanism, but it should be strongly enhanced for the twist defect case. The experiment by Flaus and Richmond [29] is related to this idea. They measured repositioning rates on DNA fragments for two types of positioning sequences, namely nucleosome A on a 242 bp fragment and nucleosome B on a 219 bp fragment, as a function of temperature. It was found that the repositioning rates depend strongly on temperature and on the positioning sequence: at 37°C it takes about 90 minutes for the A242 and more than 30 hours for the B219 to reposition half of the material. For the slower nucleosome B the set of new positions were all multiples of 10 bp apart; that is, they all had the same rotational phase. However, the faster nucleosome A did not show such a clear preference for a rotational positioning. It was argued that these differences reflect specific features of the underlying base-pair sequences: nucleosome B is complexed with a DNA sequence that has AA/AT/TA/TT dinucleotides with a 10 bp periodicity inducing a bend on the DNA, whereas nucleosome A is positioned via homonucleotide tracts. These observations are consistent with the twist defect picture where the corkscrew motion of nucleosome B is suppressed by the anisotropically bendable DNA template.

A different experimental approach was taken by Gottesfeld et al. [36]. The authors studied repositioning on a 216 bp DNA fragment that again contained the sea urchin 5S rDNA nucleosome positioning sequence, but this time in the presence of pyrrole-imidazole polyamides, synthetic minor-groove binding DNA ligands, that are designed to bind to specific target sequences. Experiments have been performed in the presence of one of four different ligands, each with one binding site on the nucleosomal DNA. It was found that a one-hour incubation at 37°C in the absence of any ligand leads to a redistribution of the nucleosomes. This redistribution was completely suppressed in the presence of 100 nM ligands *if* the target sequence of this specific ligand faces outside (toward the solution) when the nucleosomal DNA is bent in its preferred direction. On the other hand, a ligand whose binding site faces the octamer in its preferred rotational frame had no detectable effect on the reposition dynamics.

Does the outcome of this experiment determine the mechanism underlying repositioning? The ligands bind into the minor groove (see the co-crystal complexes between nucleosomes and such ligands [39]), which suggests that a bound ligand will block the overall corkscrew motion of the DNA. This is because the DNA can only rotate on the nucleosome up to a point where the bound ligand comes close to one of the 14 binding sites. This means that the observed suppression of mobility through ligand binding is consistent with the twist defect picture. But would it also be consistent with the bulge mechanism? The answer is in this case not obvious. But in a first approximation it seems plausible to assume that a bound ligand does not hinder bulge diffusion—at least sterically. A definite answer is hard because the ligand might locally alter the DNA elastic properties; nevertheless, the strong influence of ligand binding on nucleosome mobility supports the twist defect picture.

In [40] we determined the diffusion constant of a nucleosome along DNA in various cases. In our model we assume that the nucleosome in the presence of a ligand can be in three states (see Figure 7.6): the rotational setting of the wrapped DNA is such that its binding site is occluded, Figure 7.6*a*, or it is facing the solution without a ligand, Figure 7.6*b*, or with the ligand bound, Figure 7.6*c*. If we assume thermodynamic equilibrium, it is straightforward to determine the diffusion constant in the various cases. In particular, we found that for the case of a rotational position sequence with

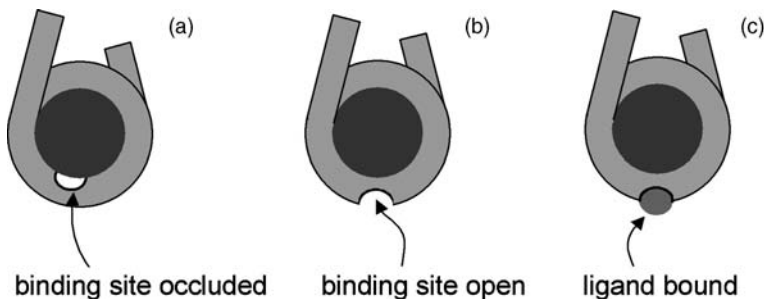


Figure 7.6 Nucleosome repositioning in the presence of DNA ligands that bind at a specific site on the nucleosomal DNA. A nucleosome can then be in three different states: (a) With its ligand binding site occluded, (b) with its binding site open, and (c) with a bound ligand. A nucleosome in state (c) cannot perform a corkscrew form of sliding.

$A \gg k_B T$ in the presence of a ligand whose binding site is exposed in the preferred rotational frame,

$$D = \frac{\pi A e^{-A/k_B T}}{k_B T} \frac{D_0}{1+K}, \quad (7.8)$$

whereas for the case of a ligand whose binding site is preferentially occluded, we have

$$D = \frac{\pi A}{k_B T} \frac{D_0}{e^{A/k_B T} + K}. \quad (7.9)$$

Here $K = [L]/K_d$ is the equilibrium constant of the ligand of concentration $[L]$ and dissociation constant K_d . Obviously in the absence of ligands $K = 0$ and (7.8) and (7.9) reduce to (7.7) for $A \gg 1$.

Equations (7.8) and (7.9) allow the influence of ligands on repositioning to be estimated for the various cases. In the following we define the typical equilibration time on a 216 bp long template (used in [36]) as $T_{70\text{bp}} = (216 - 146)^2 \text{ bp}^2 / (2D)$. For an isotropic piece of DNA we estimated above $D = D_0 \approx 580 \text{ bp}^2/\text{s}$ which leads to a typical equilibrium time $T_{70\text{bp}} = 4 \text{ s}$. If a positioning sequence is used instead with $|\Delta G_{12}| = 9k_B T$, then from (7.7) in the absence of ligands $D \approx 2 \text{ bp}^2/\text{s}$ and $T_{70\text{bp}} \approx 20$ minutes. Repositioning experiments on such sequences are thus typically performed on a time scale of an hour to ensure equilibration [26,36]. Adding now a ligand with $[L] = 100 \text{ nM}$ and $K_d = 1 \text{ nM}$ with a binding site that faces the solution in the preferred rotational frame, we can predict from (7.8) a dramatic reduction of the diffusion constant by a factor of 100: $D \approx 2 \times 10^{-2} \text{ bp}^2/\text{s}$ and $T_{70\text{bp}} \approx 34 \text{ h}$. In this case no repositioning of the nucleosomes is observed on the time scale of an hour, and this is in accordance with the experimental observations (see Figure 7.6), lane 1 and 4 in the study by Gottesfeld et al. [36]. On the other hand, for the case of a ligand with same affinity and concentration but with the binding site in the unfavorable orientation, hardly any effect is seen; in fact the diffusion constant as compared to the ligand free case is reduced by approximately 1%; see (7.9). In the experiment [36] these two cases were indeed indistinguishable (see Figure 7.5, lanes 0, 2, and 3 in that paper).

Additional experimental evidence for twist defect diffusion was provided in a recent study [41]. Edayathumangalam et al. analyzed polyamide binding to NCPs that contain either a 146 bp alpha satellite DNA sequence or a 147 bp version of the same sequence, with one additional bp at the dyad. For the latter sequence the two halves of the nucleosomal DNA have exactly the same rotational positioning with respect to the histone octamer, whereas there is a displacement by one bp between the two halves in the 146 bp NCP. Based on the polyamide binding, DNase I and hydroxyl radical footprinting, it was concluded that twist diffusion between different states does occur in solution.

In conclusion, there is strong experimental evidence that the autonomous repositioning of nucleosomes is based on twist defects. This process is slow in experiments because they are performed on DNA templates that contain nucleosome positioning sequences. However, only a small fraction of eukaryotic genomic DNA (<5% [42]) seems to contain positioning sequences. This suggests a very dynamic picture of

chromatin where the majority of nucleosomes are incessantly sliding along DNA—as long as they are not pinned to their location via linker histones [28].

Nucleosomal mobility has also profound consequences for the interaction of nucleosomes with motor proteins. Since most nucleosomes seem to be rather mobile, it might be that only positioned nucleosomes need the action of active (ATP-consuming) remodeling mechanisms [43] making them switch elements that bring about, for instance, gene activation or repression. Such chromatin remodeling complexes might catalyze the formation of twist defects or bulges. In [44] a remodeling complex induced nucleosome repositioning was found even when the DNA was nicked and a torsion could not be transmitted, suggesting that at least for this specific example active repositioning might involve loop defects.

A motor protein of special interest is RNA polymerase. During transcription of a gene, the polymerase has to “get around” tens to hundreds of nucleosomes. The interaction between RNA polymerase and nucleosomes is the subject of the next section.

7.4 TRANSCRIPTION THROUGH NUCLEOSOMES

The study by Gottesfeld et al. [36] also addressed the question how nucleosomes affect transcription. For that purpose the 216 bp DNA fragment contained a T7 promoter in addition to the 5S positioning element. The transcription reaction of the *naked* 216 bp fragment with T7 RNA polymerase produced a 199 bp full-length RNA transcript. Importantly this reaction was not affected by the presence of any of the above mentioned ligands. Even the nucleosome templates produced full-length transcripts with a very high yield, indicating that the RNA polymerase was able to overcome the nucleosomal barrier. This was also the case in the presence of ligands whose binding site faces the octamer in the preferred rotational frame. Remarkably the addition of ligands whose binding sites are open at the preferred rotational setting blocked the transcription. In fact single-round transcription assays showed that the polymerase got stuck just within the major nucleosome position. Moreover an inspection of the nucleosome positions showed that in the absence of any ligand (or in the presence of the ligands that did not block transcription) nucleosome repositioning took place. In other words, transcription did not result in a loss of the nucleosome but in its repositioning instead.

We have discussed in the previous section why nucleosomes in the presence of ligands with “open” binding sites show a dramatic reduction of their diffusion constant; see (7.8). The Einstein relation $\mu = D/k_B T$ provides a link between nucleosomal mobility μ and diffusion constant D —in the case of thermodynamic equilibrium. It is tempting to speculate that it is this difference in nucleosomal mobility that is responsible for the different outcome of the transcription experiment described in [36].

Let us begin with the case of a long DNA template with a nucleosome positioned far from any of the DNA termini. Suppose that an elongating RNA polymerase encounters such a nucleosome. If the mobility of the nucleosome is large enough, the RNA polymerase would be able to push the nucleosome in front of it—by pulling the DNA in corkscrew fashion. In the simplest mean-field type approach [40] the nucleosome will

begin to slide with a constant speed v as a result of the imposed external load F as follows:

$$v(F) = \mu F. \tag{7.10}$$

The polymerase slows down because of the force that it has to exert on the nucleosome. According to Wang et al. [45] (see also related studies [46,47]) the force–velocity relation of RNA polymerase has typically the following functional form:

$$v(F) = \frac{v_0}{1+a(F/F_{1/2})^{-1}}, \tag{7.11}$$

where v_0 is the velocity of the elongating complex in the absence of an external load and $F_{1/2}$ is the load at which the speed of the RNA polymerase is reduced to $v_0/2$. a is a dimensionless fit parameter.

In equating (7.10) and (7.11), we can determine the average speed of an RNA polymerase that pushes a nucleosome in front of it. The solution is found graphically in Figure 7.7 by determining the point of intersection between the corresponding curves (marked by circles). Curves 1 and 2 in Figure 7.7 give force–velocity relations of RNA polymerase, equation 7.11, for two sets of parameters, namely $a = 2 \times 10^4$, $F_{1/2} = 24$ pN, and $v_0 = 16$ bp/s for curve 1 and $a = 5 \times 10^4$, $F_{1/2} = 16$ pN, and $v_0 = 7$ bp/s for curve 2. These parameters have been chosen to give a good fit to the data of Wang et al. [45] for the case of *Escherichia coli* RNA polymerase in the presence of 1 mM nucleoside triphosphates (NTPs) for two different concentrations of pyrophosphate (PP_i), namely curve 1 for 1 μ M. PP_i and curve 2 for 1 mM PP_i . As was mentioned above in the experiment of Gottesfeld et al. [36], a T7 RNA polymerase was

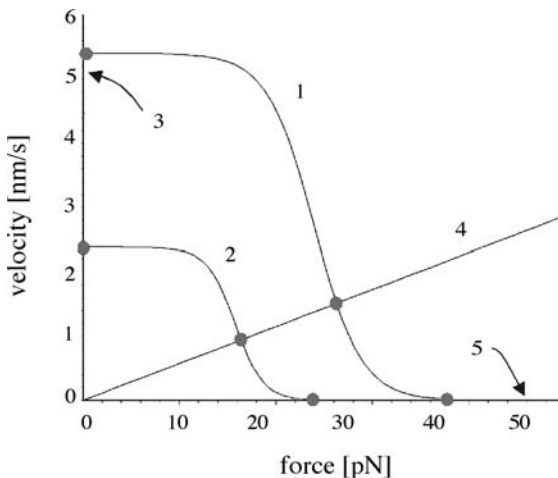


Figure 7.7 Force–velocity relations. Curves 1 and 2 show the relation between transcription-velocity and externally applied load of RNA polymerase in two different cases. Lines 3 to 5 give the force–velocity relation for nucleosomes under an externally imposed force, again for three different cases.

used and the concentration of NTPs was 250 to 500 μM . This means that curves 1 and 2 can only be considered rough estimates for the force–velocity characteristics of the T7 RNA polymerase. Curves 3 to 5 give the force–velocity relation (7.10), for the nucleosomes in various cases discussed in the previous section. Curve 3 corresponds to the case where a nucleosome slides along an isotropic DNA segment in the absence of any ligands. Curve 4 represents corkscrew sliding along an anisotropic DNA with a barrier height $9k_B T$ as it is the case for the 5S positioning sequence. Finally, curve 5 corresponds to the case where in addition to such an anisotropic bendability the mobility is slowed down by the presence of 100 nM ligands, with the ligand binding site facing the solution in the preferred DNA bending direction.

By inspecting the points of intersection among the curves, we come to the conclusion that RNA polymerase would be hardly slowed down by the presence of a nucleosome on a homogeneous track of DNA; see the point of intersection between line 3 with curve 1 (or 2) in Figure 7.7. We expect that the polymerase would easily push the nucleosome in front of it without being slowed down. On the other hand, the 5S positioning element should affect the transcription rate by a considerable amount (see line 4 and curves 1 and 2); still the RNA polymerase might be able to push the nucleosome ahead of it. Finally, in the case of added ligands the nucleosome blocks the way of the polymerase: the point of intersection between curves 5 and 1 (or 2) is close to a vanishing transcription velocity.

In the experiment [36] there is, however, an additional complication: the nucleosome is positioned at the 3'-end of the template. That means as soon as the polymerase encounters the nucleosome (here after it has transcribed the first ≈ 54 bp) it has to push the nucleosome *off* the DNA template. What is the energetic cost of this process? There are 14 binding sites between the DNA and the octamer, with a 10 bp distance between neighboring ones. As was mentioned in the introduction, the detachment of any of these 14 nucleosomal binding sites costs roughly $6k_B T$. However, the overall energetic cost of undressing the nucleosome is smaller: when pulling 10 bp off the octamer, one binding site is opened but 10 bp are released on the other side, gaining roughly $4k_B T$ elastic energy by going from the wrapped, bent state to the straight state. In total, a shift of the DNA by 10 bp costs therefore only $2k_B T$ and corresponds to a force of just 2 pN. This additional force can be easily supplied by the RNA polymerase.

Therefore our calculation leads to the prediction of the following effect of the RNA polymerase on the nucleosome: (1) In the ligand-free case the RNA polymerase is able to produce the full-length transcript pushing the nucleosome off the template. (2) If a ligand is bound to the nucleosomal DNA, the nucleosome is immobile, and the polymerase stalls as soon as it encounters the nucleosome. Whereas the second prediction is indeed in agreement with the experimental observations, the first is not. This is because that transcription was found not to lead to the loss of the nucleosome but instead to its repositioning on the template [36]. The experimental findings even indicate that the nucleosome—as a result of the transcription—is effectively moving upstream. In fact such effects have been studied in detail before and led to the proposition of a spooling mechanism [48–51] that we will discuss later in this section.

In order to explain the experimental observations of [36], we proposed in [40] a new mechanism that is depicted in Figure 7.8. (a) At the beginning of the transcription

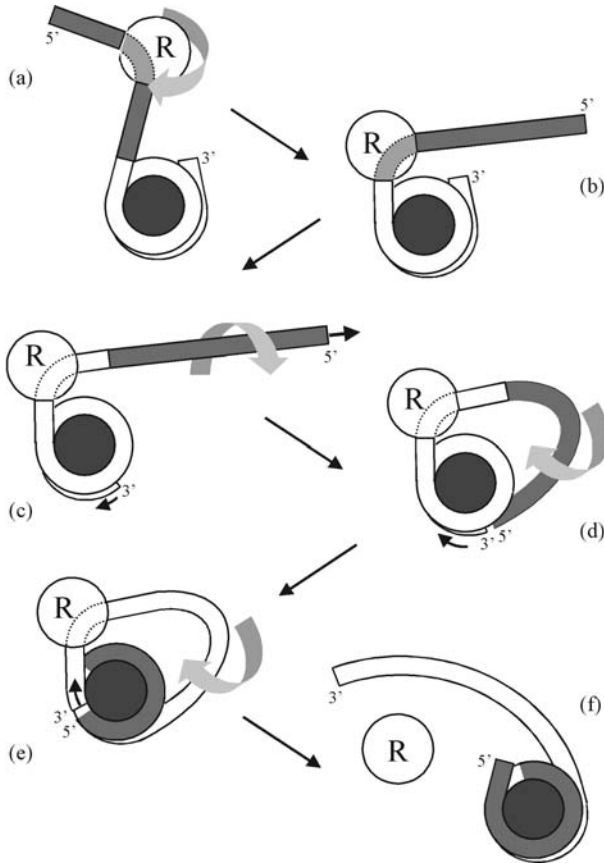


Figure 7.8 Tentative model for nucleosome repositioning via an extranucleosomal loop: The transcribing polymerase encounters in (b) the nucleosome. It gets stuck if the nucleosome is immobile or (c) it starts to pull the DNA in a corkscrew fashion from the nucleosome, “undressing” it at the other end. (d) The free DNA end adsorbs on the nucleosomal binding sites that have just been exposed. As a result an *extranucleosomal* loop has formed. (e) The RNA polymerase continues to pull the DNA around. (f) Finally the other DNA end is released. As a result of the transcription the nucleosome has been transferred to the other (former free) end of the DNA.

(the first 54 bp in [36]) the RNA polymerase walks along the free DNA section (shown in dark gray) in a corkscrew fashion. (b) The polymerase comes into contact with the nucleosome. At this stage the polymerase gets stuck if the nucleosome is immobile. (c) If the nucleosome is mobile, the polymerase pulls on the DNA, undressing the nucleosome at the other end (the 3' end). During this process the polymerase and the octamer are not moving with respect to each other, and it is only the DNA that is performing a corkscrew motion. (d) After enough nucleosomal

contact points (at the 3' end) are exposed to the solvent, the 5' end might adsorb on these contact points, forming an *extranucleosomal loop*. The loop formation probability might be increased by a kink in the DNA that is induced by the polymerase [51]. (e) The DNA continues to circle around the polymerase–nucleosome complex via the corkscrew mechanism. Note that the negative torsion in the loop, which is produced by the polymerase upstream (toward the 5' end) and the positive torsion downstream (toward the 3' end), induces the directed corkscrew motion of the wrapped DNA portions on both sides. (f) When the 3' end reaches the polymerase, this end is released from the nucleosome. An end-positioned nucleosome results again, but now it is the promoter end that is wrapped on the nucleosome. A section of the original positioning sequence (shown in white) forms the free tail.

This mechanism always transfers the nucleosome from one end of the DNA template to the other. In principle, it is also possible that a smaller loop forms with the 5' end forming an overhanging tail; see Figure 7.9. Such a small loop might be possible because the RNA polymerase induces a bend on the DNA. The RNA polymerase will then again pull the DNA around via the corkscrew mechanism. Because of the presence of the loop the 5' tail may only be able to adsorb beyond the dyad after the 3' end is released. At this point the nucleosome has effectively made a step upstream. The step length is the sum of the length stored in the loop plus the number of bp of the 3' end that were still adsorbed at the point of its release. It is possible that the 3' is released at a point where it was still associated with a few binding sites (each binding site just contributes on the order of $2k_B T$). The typical upstream step length is then a few tens of bp. An interesting feature of this variant of the model is that the step length should not depend on the length of the originally free DNA portion (shown in dark gray in Figure 7.9). In other words, if the nucleosome is

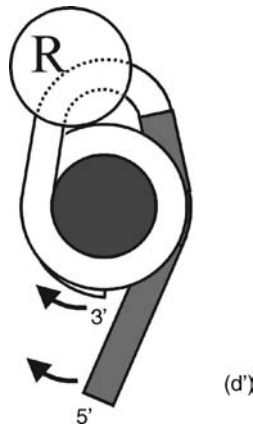


Figure 7.9 Alternative version of the extranucleosomal loop model: In stage (d) of Figure 7.8 the bend induced by the RNA polymerase leads to the formation of a very small extranucleosomal loop. The 5' end forms then a tail on the nucleosome.

initially positioned at one end of the template (due to some positioning sequence), after transcription it is shifted upstream to a new position by a distance that is independent of the length of the DNA template.

The experiment by Gottesfeld et al. [36] showed that nucleosomes survive transcription, but it is not possible to deduce from the data whether transcription through a nucleosome leads to its repositioning along DNA. There is, however, a long series of experiments that have focused on this point [48–51]. Also in these experiments a bacteriophage RNA polymerase has been used, namely that of SP6. The standard 227 bp template includes an SP6 promoter and a nucleosome positioning sequence [48]. Typically the nucleosome is positioned at the promoter distant end. Transcription results in an upstream displacement to the other end, namely by 80 bp [48]. Whether this step length reflects a built-in step length of the repositioning process or whether the nucleosome is displaced from one end to the other has been checked by adding an extra length to the DNA template at either end. Adding extra 50 bp at the promoter side (the 5' end) the upstream step is typically 90 bp; that is, it does not increase much. This might indeed indicate that the displacement process has a natural 80 to 90 bp step length. On the other hand, addition of 35 bp to the 3' end has surprisingly also an effect on the upstream step length that shows now three smaller values, namely 40, 60, and 75 bp [48]. Finally, going to a much larger template by adding 126 bp at the promoter end led to another surprise: In this case the nucleosome is transferred from one end to the other as a result of the transcription [49].

How can these observations be rationalized? Studitsky et al. [48] Introduced the “spooling” mechanism (see their Figure 7.7): as the polymerase encounters the nucleosome, it continues to transcribe by prying off the DNA from the octamer. After the polymerase has proceeded far enough into the nucleosomal DNA, the DNA behind the polymerase might attach to the now exposed nucleosomal binding sites. This results in an *intranucleosomal* loop. The polymerase travels around the nucleosome inside this loop. On reaching the other end, the loop disappears, and as a result the nucleosome steps upstream by the extra DNA length that has been stored in that loop. The step lengths observed in the experiments have then to be interpreted as the loop sizes. A preferred value would be around 80 bp. Studitsky et al. explained the much shorter step lengths observed in the case of a template with a DNA extension on the promoter distant site as a result of “octamer slippage” before the spooling mechanism comes into play with the usual 80 bp upstream step. Finally, the end-to-end transfer on the long 353 bp template indicates a large loop that stores 180 to 200 bp [49].

These observations and their explanation are in fact entirely consistent. One should nevertheless ask whether our *extranucleosomal* loop model provides also a picture consistent with these experimental facts. The model depicted in Figure 7.8 even predicts an end-to-end transfer of the nucleosome as it has been observed for the longest template discussed above. The modified model with a small *extranucleosomal* loop, as depicted in Figure 7.9, leads to a smaller upstream step of the octamer whose value depends on microscopical details but should be on the order of a few tens of bp. So this picture could also explain the typical 80 bp shifts observed in several cases.

This leads us to the surprising conclusion that either mechanism, the extra- and the intranucleosomal one, is consistent with the observations. It is only the smaller steps where Studitsky et al. suggested octamer slippage to occur that might ironically speak in favor of their model. When the nucleosome steps back by 40 bp, it might have first slid 35 bp to the 3' end and then have gone back by 80 bp with either mechanism. However, the fact that after transcription some nucleosomes were found 60 and 75 bp upstream might support the intranucleosomal loop picture: first the nucleosome slides a short distance (but not up to the DNA terminus) and then steps back by 80 bp due to an intranucleosomal loop. Still it seems impossible to exclude from these experimental observations one or the other mechanism, and it might well be the case that both play a role.

Another feature that has been observed during the transcription “through” nucleosomes is a characteristic pausing pattern of the polymerase [49,52]. Studitsky et al. [49] reported for SP6 RNA polymerase a pausing with a 10 bp periodicity that disappears once the transcription has progressed beyond the nucleosomal dyad. Protacio et al. [52] find pausing with this periodicity, however, extending far beyond the dyad. The ladder system uses T7 RNA polymerase and the 5S positioning element as in [36]. Studitsky et al. interpret their observations with their spooling model: once the loop has formed, the polymerase might not be able to continue with elongating because it would have to rotate through the loop, and this process might be too costly if not even sterically forbidden. Instead pausing occurs up to the point when the loop reopens through a spontaneous fluctuation. The loop formation (and the concomitant pausing) might happen with a 10 bp periodicity since the bend induced by the polymerase can help the loop formation every 10 bp. Once the dyad has been reached, the last loop forms that is finally broken *ahead* of the polymerase, allowing the polymerase to transcribe from now on without interference from the octamer. Further support for this idea was given by removal of DNA behind elongating complexes that had been arrested just at the nucleosomal border. Resuming transcription, the polymerase was able to elongate into the nucleosome much further without pausing before it encountered a first pausing site. This was interpreted again as a fact supporting the spooling model [49]: the formation of the loop was only possible when enough DNA was available at the 5' end.

We believe that these observations are also consistent with the extranucleosomal loop picture. The 10 bp pausing pattern might reflect the 10 bp periodicity of the bending energy of the positioning sequence. Enhanced pausing might occur once the loop has formed because of the enhanced friction of the corkscrewing DNA. And the disappearance of pausing sites beyond the dyad (which is not for all situations the case; see [52]) might reflect the termination of an interaction between the polymerase and DNA wrapped close to the dyad. In case of the 5' end forming a tail, as shown in Figure 7.9, this end might not be able to adsorb beyond the dyad as long as the intranucleosomal loop is present, so the friction or entanglement between the components decreases once the polymerase passes the dyad.

This brings us to the next point of our discussion. One might wonder whether such intra- or extranucleosomal loops can be directly “seen” in electron micrographs. In fact cryomicroscopy has been performed for such complexes [51]. Unfortunately, also here

the situation is rather complex. When the polymerase was arrested after transcribing 23 bp into the nucleosome, the electron cryomicrographs showed complexes with one DNA tail. The length of that tail was considerably longer than the tail in the absence of RNA polymerase. This was interpreted as being due to a polymerase-induced DNA unwrapping. Interestingly our corkscrew sliding scenario also leads to a tail lengthening without the necessity of DNA unpeeling; see Figure 7.8c. The polymerase was also arrested further into the nucleosome (42 bp), a location at which intra- or extranucleosomal loops should be expected. Loops were, however, not observed (at least not large ones); instead there was a considerable fraction of two-tailed intermediate states. These closed transcription intermediates were interpreted as states that resulted from the collapse of an internucleosomal loop; see Figure 7 in [51]. In our opinion, such an explanation (being an attempt to reconcile the spooling model with the two-tail intermediates) is not obvious, even though this picture cannot be excluded. On the other hand, when the polymerase is stalled after a small extranucleosomal loop has formed, two-tail intermediates should be expected. In Figure 7.9 the 5' end is forming the only tail. But it is even possible that the 3' desorbs up to the dyad where the loop blocks further unpeeling. This then leads to two-tail complexes where both ends form tails of varying lengths.

The experiments of Studitsky et al. [48–51] are indeed compatible with their spooling model. However, as argued above, our extranucleosomal loop mechanism gives a consistent explanation of their experiments. Only the recent observation by Gottesfeld et al. [36] of transcription blockage via ligands votes strongly for the extranucleosomal loop mechanism. It should be noted that the experimental conditions (e.g. type of polymerase) are different in this case. This still leaves space for the possibility that different mechanisms for transcription through nucleosomes could occur in the various cases.

We note that the two different scenarios involving intra- and extranucleosomal loops lead to dramatically different pictures for transcription on multinucleosomal templates. Whereas the elongating RNA polymerase could easily get around all the nucleosomes via intranucleosomal loops, our extranucleosomal variant relies on the finite length of the DNA. This mechanism would cease to work for the multinucleosomal situation. Transcription on reconstituted multinucleosomal templates showed indeed that T7 RNA polymerase is under certain conditions capable of disrupting completely the nucleosomal cores [53,54]. Electron micrographs show the transcribed section to be freed of nucleosomes and parts of the histones being transferred to the nascent RNA chain [54]. Interestingly upon addition of some nuclear extract the nucleosomal template seem to survive during transcription [53]. This shows that the *in vivo* situation might be more complex and involve additional factors mediating between polymerase and nucleosomes.

7.5 TAIL BRIDGING

Up to now we have discussed single nucleosomes. In a cell, however, each DNA chain is complexed with millions of octamers distributed along the chain with a repeat length

of roughly 200 bp [5]. A fiber with a 30 nm diameter, the chromatin fiber, is typically posited as the structure emerging from this string of nucleosomes [55]; see also level 3 in Figure 7.1. In this fiber, and also in higher order structures beyond it, nucleosome–nucleosome interaction plays a crucial role.

The chromatin fiber has a contour length that is about 40 times shorter than that of the DNA chain it is made from. But at the same time the fiber is much stiffer than the naked chain, so that its coil size in a dilute solution will be much larger than the diameter of the cell nucleus. Specifically the size of a stiff polymer chain with persistence length l_p , diameter D , and contour length L in a good solvent scales like $R \approx l_p^{1/5} D^{1/5} L^{3/5}$ [56]. A human chromosomal DNA chain has $L \approx 4$ cm. This together with $l_p = 50$ nm and an effective diameter $D \approx 4$ nm (assuming physiological ionic conditions) leads to $R \approx 100 \mu\text{m}$. On the other hand, the chromatin fiber has $L \approx 1$ mm, $l_p \approx 200$ nm [57–59] and $D \approx 30$ nm leading to $R \approx 20 \mu\text{m}$. There are 46 chains that have to fit into the nucleus with a diameter of 3 to 10 μm . This clearly calls for the necessity of nucleosome–nucleosome attraction as a further means of compaction. This mechanism should be tunable such that fractions of the fiber are dense and transcriptionally passive, while others are more open and active.

This suggests the following questions: Do nucleosomes attract each other, and what is then the underlying mechanism? Can this interaction be tuned for individual nucleosomes? And can this be understood in simple physical terms? Recent experiments indeed point toward a simple mechanism for nucleosomal attraction: histone tail bridging [60–62]. As was mentioned in the introduction, the histone tails are flexible extensions of the eight core proteins that carry several positively charged residues and whose lengths range from 15 residues (histone H2A) to 44 (H3). These tails extend considerably outside the globular part of the nucleosome, as sketched schematically in Figure 7.2. Mangelot et al. [60] studied dilute solutions of NCPs. Using small angle X-ray scattering, they demonstrated that NCPs change their size with salt concentration. At around 50 mM monovalent salt the radius of gyration increases slightly (from 43 to 45 Å), but at the same time the maximal extension of the particle increases significantly (from 140 to 160 Å). This was attributed to the desorption of the cationic histone tails from the NCP that carries an overall negative charge (see [5]). Osmometric measurements [61] detected around the salt concentration where the tails desorb an attractive contribution to the interaction between the NCPs, reflected in a considerable drop of the second virial coefficient. The coincidence of the ionic strengths for the two effects led Mangelot et al. to suggest that it is the tails that are mainly responsible for the attractive interaction. This picture is supported by the experimental fact that the attraction disappears once the tails are removed from the NCP [62].

Theories for nucleosomal attraction come to diverging conclusions. Attraction between simplified model nucleosomes has been reported in a nucleosome model [63,64] that ignored the tails. The nucleosome was modeled by a positively charged sphere (representing the protein core) and a negatively charged semiflexible chain (modeling the DNA) wrapped around it. The interaction between two such complexes (at zero temperature) showed an attraction at intermediate salt concentrations that leads to nonmonotonic behavior of the second virial coefficient with the minimum

reflecting the attractive regime (see Figure 4 in [63]). In a more general context this kind of nonmonotonic interaction can be interpreted to belong to the class of attraction induced by correlations between charge patches [65]. An example is a computer simulation of Allahyarov et al. [66] who studied the interaction between spherical model proteins decorated with charge patches; the second virial coefficient featured nonmonotonic behavior as a function of ionic strength.

On the other hand, Podgornik [67] focused on tail bridging in a model where the NCP was represented by a point-like particle with an oppositely charged flexible chain. This system showed NCP–NCP attraction but no nonmonotonic behavior of the second virial coefficient. Thus the question arises whether it is really the tail bridging that causes the attraction between NCPs observed at intermediate salt concentrations. Earlier studies had already established that polyelectrolyte chains form bridges between charged planar surfaces [68,69] and colloids [70,71] (carrying charges of a sign opposite of that of the chains) that cause attraction. An interesting demonstration of the difference between attraction due to charge correlations and due to bridging was given by continuously changing the stiffness of the entropic springs connecting neighboring monomers of the polyelectrolyte chains [68]: a vanishing spring constant leads to the usual repulsive double-layer force due to the counterions in between the walls, harder springs lead to polyelectrolyte chains that cause bridging, and finally very hard springs induce a collapse of each chain onto a point that corresponds to multivalent counterions whose charge correlations cause attraction. Both effects, bridging and charge correlations, lead to attractive regimes that were clearly separated from each other (e.g., see Figure 8 in [68]). Of interest is also the observation that bridging interactions induced by free chains are very similar to those of chains that are grafted on either surface [69].

Although those earlier studies provide already substantial insight into bridging interactions, several issues remained open, especially in the light of the new experimental [60–62] and theoretical studies [63,64,66]. A recent paper [72] introduced a minimal model for NCPs that includes its tails to test whether such a model shows attraction with a nonmonotonically varying second virial coefficient. This model puts tail bridging on a stronger footing in demonstrating how the ensuing effect is qualitatively different from attraction through charge patches, and how tail bridging can be used to facilitate control of nucleosomal interaction. Such control might in turn affect the compaction state of chromatin.

That NCP model, called the eight-tail colloid, is depicted in Figure 7.10. It consists of a sphere with eight attached polymer chains. The sphere is a coarse-grained representation of the NCP without the tails, meaning the globular protein core with the DNA wrapped around. The sphere carries a central charge Z that represents the net charge of the DNA–octamer complex. Because the DNA overcharges the cationic protein core, the charge is $Z < 0$ [5]. Furthermore the sphere radius is chosen to be $a = 15\sigma$ with $\sigma = 3.5$ Å being the unit length. The eight-histone tails are modeled by flexible chains grafted onto the sphere (at the vertices of a cube). Each chain consists of 28 monomers of size σ where each third monomer carries a positive unit charge, the rest being neutral. All these parameters have been chosen to match closely the values of the NCP; for example, the tails feature the average length of the N-terminal tails. The

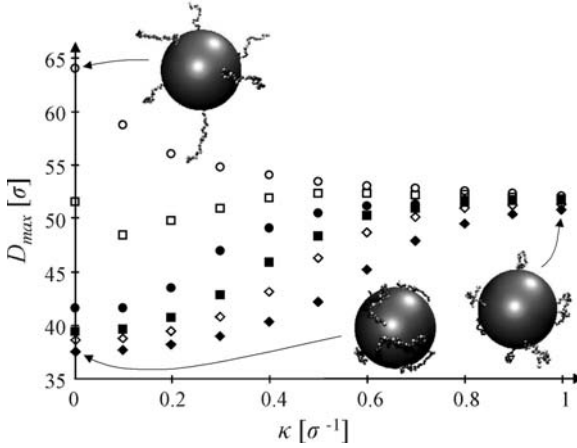


Figure 7.10 Average maximal extension of the eight-tail colloid as a function of the salt concentration, together with three example configurations. The different curves correspond to different values of the central charge: $|Z|=0$ (open circles), 50 (open squares), 100 (filled circles), 150 (filled squares), 200 (open diamonds), and 300 (filled diamonds).

simulations were performed in a NVT ensemble using a Langevin thermostat [73] with a time step of 0.01τ and a friction coefficient $\Gamma = \tau^{-1}$ (Lennard-Jones time unit). The hard cores were modeled with a purely repulsive Lennard-Jones potential [74], and the chain connectivity with a finitely extensible nonlinear elastic (FENE) potential [74]; the central sphere was allowed to freely rotate. In addition all charged monomers and the central sphere experience an electrostatic interaction via the standard Debye–Hückel (DH) theory with an inverse screening length $\kappa = \sqrt{4\pi l_B c_s}$, where c_s denotes the monovalent salt concentration and $l_B = 2\sigma$ sets the Bjerrum length in water at room temperature ($l_B = e^2/\epsilon k_B T$, where e : electron charge; ϵ : dielectric constant of solvent) [75]. Since a DH potential was used, an effective value Z_{eff} for the central charge was needed to account for charge renormalization [76].

Figure 7.10 presents results from a molecular dynamics simulation of a single eight-tail colloid. Depicted is the thermally averaged maximal extension of the colloid as a function of κ for different values of the central sphere charge Z . For $Z=0$ and small values of κ (i.e., at low ionic strength), the eight tails are extended, radially pointing away from the center of the complex; see the example at $\kappa\sigma=0$. For large values of $|Z|$, say, for $|Z|>100$, and small κ , the tails are condensed onto the sphere; see the configuration at $|Z|=300$ and $\kappa\sigma=0$. Increasing the screening leads in both cases finally to structures where the chains form random polymer coils as in the example at $\kappa\sigma=1$. With increasing values of $|Z|$, the swelling of initially condensed tails sets in at larger κ -values. A comparison of the curves for $|Z|>100$ with the experimental ones [60] shows a qualitatively similar chain unfolding scenario. Furthermore, for $Z=-150$, the experimental and the simulation values of c_s at which tail unfolding takes place match. This value of Z_{eff} was then chosen in what follows.

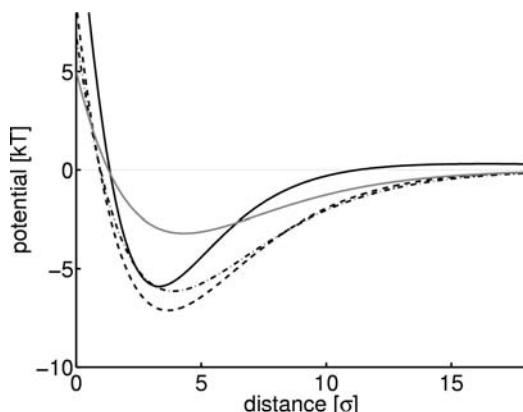


Figure 7.11 Interaction potential between two eight-tail colloids as a function of the surface–surface separation for four different values of κ : $\kappa\sigma = 0.2$ (dashed-dotted line), $\kappa\sigma = 0.3$ (dashed line), $\kappa\sigma = 0.4$ (solid line), and $\kappa\sigma = 0.6$ (gray line).

The interaction between two such complexes was determined by measuring the thermally averaged force at different distances and by interpolating the force–distance curve via a suitable least-square fit. Integration yields the pair potentials depicted in Figure 7.11 for four different values of κ . An attractive potential with a minimum of a few $k_B T$ in all four cases was found. The depth of the potential shows a nonmonotonic dependence on κ with a maximal value around $\kappa\sigma = 0.3$. This in turn is reflected in a nonmonotonic dependence of the second virial coefficient A_2 , depicted in Figure 7.12, with a minimum around the κ -value where tail unfolding occurs, namely the curve for $Z = Z_{eff} = -150$ in Figure 7.10. Again, all these observations are qualitatively similar to the experimental ones [61].

Next was studied whether this attraction can be attributed to the tail-bridging effect. In Figure 7.13a comparison of the full eight-tail model with simplified variants is

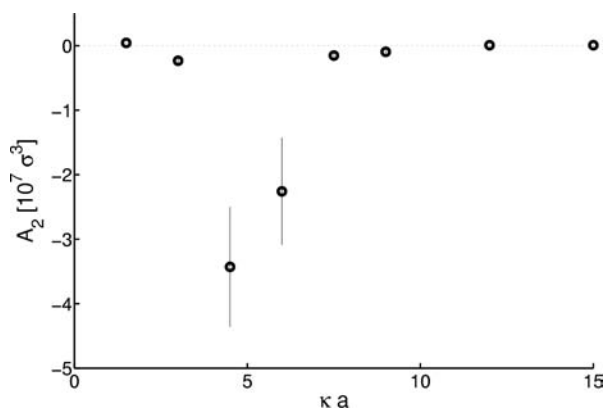


Figure 7.12 Second virial coefficient of the eight-tail colloid as a function of $\kappa\alpha$. Note the drop in A_2 at intermediate salt concentrations around $\kappa\alpha = 5$.

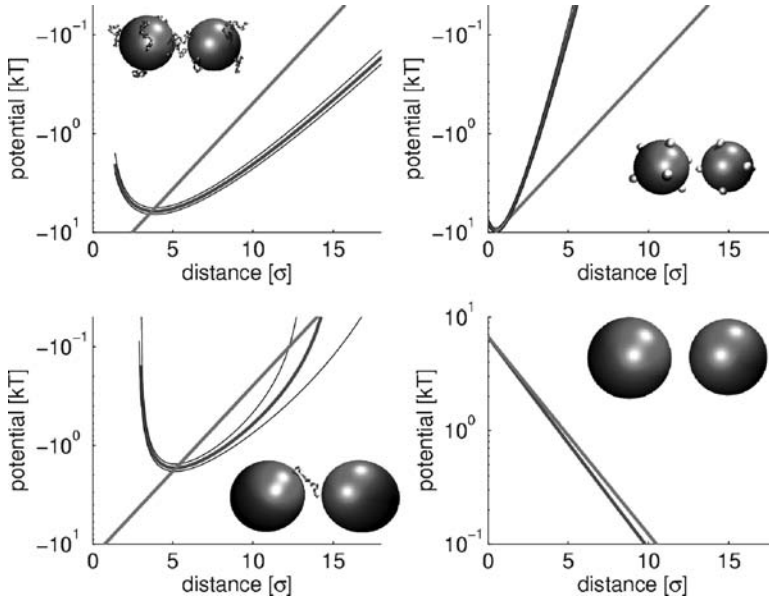


Figure 7.13 Comparison of the interaction potential (with error corridor) for four different colloids at $\kappa\sigma = 0.4$: Eight-tail colloids (*top left*), colloids with charge patches (*top right*), one-tail bridging (*bottom left*), and homogeneously charged balls (*bottom right*). For each model is depicted the potential in a semilogarithmic plot (only the attractive part for the three first cases). The curves are compared to a line with slope $\pm\kappa$.

depicted. In all cases $\kappa\sigma = 0.4$, a value close to that where A_2 has its minimal value in Figure 7.12; $\kappa\sigma = 0.4$ corresponds to 100 mM monovalent salt, which is to physiological conditions. In one case (top right) each chain is collapsed into a small patch modeled as a grafted monomer that carries the whole chain charge. Also this case shows a nonmonotonic behavior of A_2 on c_s (data not shown) so that this feature is not a criterion to use in distinguishing between tail bridging and attraction via patchiness. But by inspecting the attractive part of the pair potential, we can see that the patch model has a very rapidly decaying interaction with a slope larger than the reference line with slope κ . In sharp contrast, the eight-tail complex has a decay constant that is smaller than κ (see the top left of Figure 7.13), an effect that can only be attributed to tail bridging. This effect can also be seen for a third variant (bottom left) where 15 of the 16 tails have been removed and Z has been adjusted so that the net charges of the complexes are unchanged. The remaining one-tail complex is not allowed to rotate, so the grafting point of the chain always faces the other ball. Also in that case the range of attraction is longer than expected from pure screened electrostatics. Finally, on the bottom right the trivial case of two charged balls (with the same net charge as the full model) is presented where only a *repulsive* interaction remains.

Figure 7.14 presents a closer look at the tail-bridging effect between two eight-tail colloids, again for $\kappa\sigma = 0.4$. Depicted is the monomer distribution of bridge-forming chains that are defined as chains that have at least one of their monomers closer than a

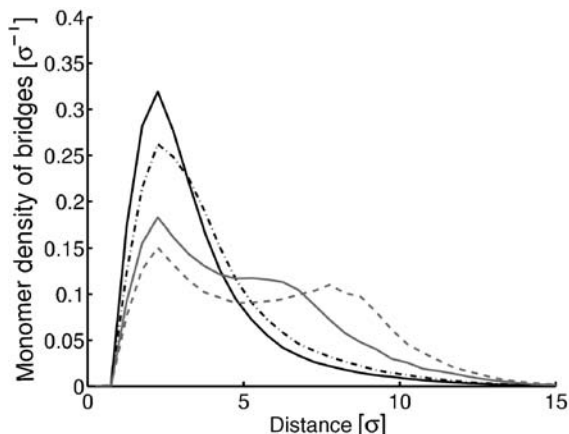


Figure 7.14 Density distribution of monomers belonging to bridge-forming tails as a function of the distance from the surface of the colloid to which the tail is grafted. The different distributions correspond to different surface–surface separations between colloids: $d = 0\sigma$ (solid), $d = 4\sigma$ (dashed-dotted), $d = 7\sigma$ (gray), and $d = 9\sigma$ (dashed).

distance 3.6σ to the surface of the alien core. For very small distances between the colloids there are almost always bridges. Their monomer distribution shows a strong peak around a distance 3σ . However, also at much larger distances like $d = 7\sigma$ and $d = 9\sigma$ there is still a considerable fraction of configurations that show bridges. Their monomer distribution shows a bimodal distribution with the two peaks clearly reflecting the condensation of monomers on the home core and the alien core. Figure 7.15 shows the interaction force between two colloids (circles) and the contributions of tail-bridging configurations (squares) and configurations without bridges (diamonds) to this force. It can be clearly seen that the tail-bridging config-

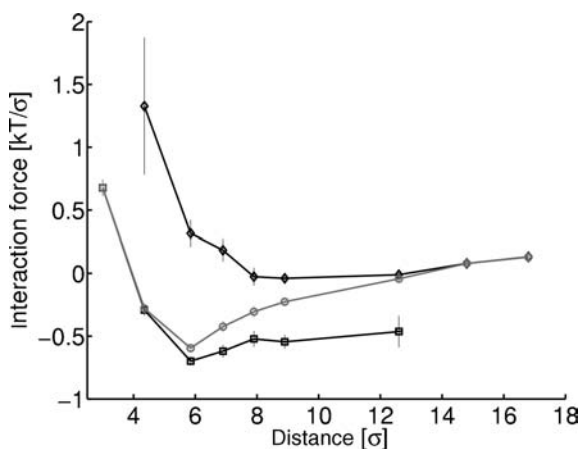


Figure 7.15 Total average of the interaction force (circles) separated into average forces stemming from configurations with bridges (squares) and nonbridging configurations (diamonds).

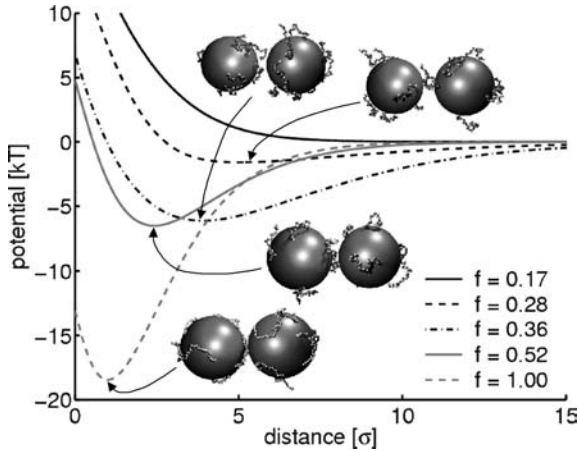


Figure 7.16 Interaction potential between two eight-tail complexes as a function of the surface–surface separation for $\kappa\alpha = 0.4$ and various charge fractions f . Also shown are examples of configurations at the equilibrium distances.

urations account to an overall attractive force, whereas in the other case the interaction is on average purely repulsive.

Up to now the tails are 28 monomers long with each third monomer being charged. As a result each tail carries 10 charged monomers, leading to a charge fraction $f = 10/28 \approx 0.36$. The role of the charge fraction for the interaction between eight-tail colloids is studied next. Figure 7.16 shows the pair interaction between two colloids as a function of distance for different values of f . The overall picture is the following: with increasing f the minimum of the pair potential becomes deeper and moves to smaller distances. Remarkable is especially how sensitive the depth of the pair potential depends on f : the potential depth for our canonical value $f = 0.36$ is around $-5k_B T$ and that for $f = 0.28$ is around $-1k_B T$, so the reduction by two monomer charges per tail nearly erases the minimum. In fact for $f = 0.17$ the minimum has totally disappeared.

The experiments on histone tail bridging [60–62] as well as the study in [72] presented here focus on the interaction between NCPs. In the cell, however, nucleosomes are connected to each other via linker DNA, which results in a chromatin fiber. This leads to the question whether tail bridging is also important for nucleosomes in such a fiber. This is indeed supported by a recent computer simulation [77] where the NCP crystal structure has been mimicked by a cylinder with 277 charge patches (accounting for charged groups on the surface of the NCP) with all the tails anchored to it. By switching on and off the charges on the tails, it was found that the tails play a crucial role in the electrostatic nucleosome–nucleosome and nucleosome–linker DNA interaction within that chromatin fiber model, causing the stabilization of the fiber at physiological salt conditions.

As shown above, tail bridging is very sensitive to the number of charges on the tails, which immediately suggest a possible mechanism to control the interaction between nucleosomes. It is known that the cellular machinery is capable of controlling the

charge state of the histone tails via the acetylation (the “discharging”) and deacetylation (the “charging”) of its lysine groups [78]. Active, acetylated regions in chromatin are more open, inactive, deacetylated regions that tend to condense locally and on larger scales as well [79]. The role of acetylation for genetic expression has been recently demonstrated via an *in vivo* experiment [80] on yeast strains that contained mutated H4 tails whose lysines were replaced by arginines that cannot be neutralized. The gene expression of these mutants had been screened for all possible combinations. Only one of the four lysine residues in the H4 tail showed a very specific response, presumably recruiting special modification-specific proteins that in turn silence, for instance, a whole region of chromatin. Mutations on the other three residues showed an unspecific, cumulative effect, suggesting that most lysines act as “charge-counters,” (i.e., the more mutations have been introduced, the stronger are the changes in gene expressions). Here are especially clustered chromosomal regions of interest where genetic activity is down-regulated with increasing charge numbers on the tails. This might reflect condensation of the chromatin fibers due to enhanced nucleosomal attraction via tail bridging in those regions.

7.6 DISCUSSION AND CONCLUSION

In this chapter we presented simple model representations of the nucleosome that allow some of its physical properties to be understood. Modeling the nucleosome via a cylinder that exerts a short-range attraction to a semiflexible chain seems to be a reasonable approximation to use for understanding the unwrapping of the nucleosome under an externally imposed tension. During the unwrapping the nucleosome has to flip by 180° , and that leads to an energetically costly transition state with highly bent DNA portions. This mechanism can explain the dramatic rupture events observed in the experiments [13]. But even more: in order to explain the force spectroscopic data, we are led to the conclusion that there must be a first-second turn difference [18] of the wrapped DNA portion as a result of an effective repulsion between the two turns. This effect might explain why the site exposure mechanism [6,7] that allows transient access for DNA binding proteins to nucleosomal DNA does not lead to the complete disruption of the nucleosome: thermal unwrapping stops once one turn is left on the nucleosome, since that remaining turn has a firm grip on the octamer. This way the two-turn design makes the nucleosome accessible to DNA binding proteins and yet assures its stability.

To describe nucleosome sliding along DNA, one needs to use a more refined model of the nucleosome that takes into account the discrete binding sites between DNA and the octamer as well as the twist and stretch rigidity of the DNA [35]. The mobility of nucleosomes can then be understood as being the result of small twist defects on the nucleosomal DNA that spontaneously form at the termini of the wrapped portion and that then propagate to the other end. That the nucleosomal mobility comes about via larger loops or bulges seems to be less consistent with recent experimental data using synthetic DNA ligands [36]. A sliding nucleosome—mobilized through twist defects—performs a corkscrew motion along the DNA, thereby, probing the intrinsic

curvature of DNA. That is why nucleosomes are substantially slowed down or even get stuck at nucleosome positioning sequences.

We discussed next whether RNA polymerase can transcribe through nucleosomes. The analysis of this problem is based on the previous model that describes nucleosome sliding through twist defects. The estimated numbers indicate that the polymerase should be strong enough to push a nucleosome in front of it, this being—at first sight—incompatible with experiments on short DNA templates where RNA polymerase seems to transcribe through a nucleosome [48]. We presented as a possible explanation a finite size effect (see Figure 7.8). This leaves the question open of how RNA polymerase can read out a gene that is covered with tens or hundreds of nucleosomes.

Finally, we focused on the role of the histone tails. To understand the basic physics of the attraction between nucleosome core particles (NCP), we suggest that it is—as a first step—sufficient to model them as negatively charged balls with positively charged tails attached [72]. By this simple model there can be reproduced qualitatively several properties of NCPs such as the unfolding of the tails with increasing ionic strength [60] and the attraction between NCPs around the same ionic conditions [61]. The mechanism underlying this attraction is tail bridging where at least one tail of one NCP bridges to the other NCP. Since tail bridging is strongly dependent on the charge state of the bridging tail, we speculate that acetylation of histone tails reduces nucleosomal attraction, making acetylated chromosomal regions more open and presumably more active.

Clearly, it would be desirable to have a nucleosome model at hand that carries all the above-mentioned features at the same time. This might, for instance, allow estimates to be made of the role of histone tails in inducing the first-second round difference of the two DNA turns and in determining the dynamics of spontaneous DNA unwrapping. Having a grip on this dynamics would make it possible, for example, to check whether the opening fluctuations on the nucleosome have an impact on the repositioning rate via twist defects.

But much more important might be to develop a model that acknowledges the fact that the octamer is not just one unit but an aggregate of a H3-H4 tetramer and two H2A-H2B dimers. For instance, even around physiological ionic conditions the nucleosome might lose its dimers once the concentration of nucleosomes is too small. The recent study by Claudet et al. [17] shows, for instance, that the unwrapping data have to be taken with care. It is not always clear whether one unwraps DNA from an entire octamer or whether under the given conditions there are mainly tetramers left. If there are only tetramers present, this might explain why the discrete unwrapping events correspond usually to the release of the last turn whereas there is no discrete unwrapping associated to the first turn. In fact, for an entire nucleosome a double-flip unwrapping might be expected with two discrete peaks per nucleosome in the force–extension curve. We suggest, however, that the first peak is not detectable because the corresponding DNA is much weaker adsorbed (first-second round difference) and because in this case the height difference between entering and exiting DNA is much larger, which also considerably lowers the barrier against unwrapping of that turn. This issue certainly deserves more work on the experimental and theoretical side.

What is even more important: It is almost certain that the tripartite nature of the octamer affects its functioning *in vivo*. Just to name one example, the “transcription through nucleosomes” discussed in Section 7.4 leaves the nucleosome intact only for bacteriophage RNA polymerase but not for eucaryotic RNA polymerase II where the nucleosome looses one dimer [81]. Even though the use of short DNA templates might lead to serious artefacts—as we have pointed out above—this observation suggests that eucaryotic RNA polymerase is prone to destroy the octameric integrity, and this might be important for its working *in vivo*.

A physical model of the nucleosome that includes as simple as possible the composite nature of the protein core might help our understanding of how the nucleosome can manage to perform all its demanding tasks. Now may be the time to bid a farewell to the “tuna-can octamer” [82].

ACKNOWLEDGMENT

We have greatly benefited from our collaborations with Robijn Bruinsma, Bill Gelbart, Jon Widom, Frank Mühlbacher, Christian Holm, Farshid Mohammad-Rafiee, Boris Mergell, and Ralf Everaers. We also wish to acknowledge helpful discussions with John van Noort, Jan Bednar, Cyril Claudet, Andrew Flaus, Stephanie Mangenot, Kurt Kremer, Rudi Podgornik, Jörg Langowski, Nikolay Korolev, Jordanka Zlatanova, Sanford Leuba, and many others. We thank Sabina Pepé Sciarria for assistance in preparing this manuscript.

REFERENCES

- [1] B. Alberts, D. Bray, J. Lewis, M. Raff, K. Roberts, J. D. Watson. *Molecular Biology of the Cell*. Garland, New York, 1994.
- [2] K. E. van Holde. *Chromatin*. New York, Springer, 1989.
- [3] K. Luger, A. W. Mäder, R. K. Richmond, D. F. Sargent, T. J. Richmond. Crystal structure of the nucleosome core particle at 2.8 Å resolution. *Nature (London)* 389 (1997): 251–260.
- [4] C. A. Davey, D. F. Sargent, K. Luger, A. W. Maeder, T. J. Richmond. Solvent mediated interactions in the structure of the nucleosome core particle at 1.9 Å resolution. *J. Mol. Biol.* 319 (2002): 1097–1113.
- [5] H. Schiessel. The physics of chromatin. *J. Phys. Condens. Matter* 15 (2003): R699–R774.
- [6] K. J. Polach, J. Widom. Mechanism of protein access to specific DNA sequences in chromatin: A dynamic equilibrium model for gene regulation. *J. Mol. Biol.* 254 (1995): 130–149. K. J. Polach, J. Widom. A model for the cooperative binding of eucaryotic regulatory proteins to nucleosomal target sites. *J. Mol. Biol.* 258 (1996): 800–812.
- [7] J. D. Anderson, J. Widom. Sequence and position-dependence of the equilibrium accessibility of nucleosomal DNA target sites. *J. Mol. Biol.* 296 (2000): 979–987.
- [8] P. J. Hagerman. Flexibility of DNA. *An. Rev. Biophys. Biophys. Chem.* 17 (1988): 265–286.
- [9] R. A. Harris, J. E. Hearst. On polymer dynamics. *J. Chem. Phys.* 44 (1966): 2595–2602.

- [10] T. J. Richmond, C. A. Davey. The structure of DNA in the nucleosome core. *Nature (London)* 423 (2003): 145–150.
- [11] F. Mohammad-Rafiee, R. Golestanian. Elastic correlations in nucleosomal DNA structure. *Phys. Rev. Lett.* 94 (2005): 238102–1–4.
- [12] K. Luger, T. J. Richmond. The histone tails of the nucleosome. *Curr. Opin. Genet. Dev.* 8 (1998): 140–146.
- [13] B. D. Brower-Toland, C. L. Smith, R. C. Yeh, J. T. Lis, C. L. Peterson, M. D. Wang. Mechanical disruption of individual nucleosomes reveals a reversible multistage release of DNA. *Proc. Natl. Acad. Sci. USA* 99 (2002): 1960–1965.
- [14] Y. Cui, C. Bustamante. Pulling a single chromatin fiber reveals the forces that maintain its higher-order structure. *Proc. Natl. Acad. Sci. USA* 97 (2002): 127–132.
- [15] M. L. Bennink, S. H. Leuba, G. H. Leno, J. Zlatanova, B. G. de Grooth, J. Greve. Unfolding individual nucleosomes by stretching single chromatin fibers with optical tweezers. *Nat. Struct. Biol.* 8 (2001): 606–610.
- [16] L. H. Pope, M. L. Bennink, K. A. van Leijenhorst-Groener, D. Nikova, J. Greve, J. F. Marko. Single chromatin fiber stretching reveals physically distinct populations of disassembly events. *Biophys. J.* 88 (2005): 3572–3583.
- [17] C. Claudet, D. Angelov, P. Bouvet, S. Dimitrov, J. Bednar. Histone octamer instability under single molecule experiment conditions. *J. Biol. Chem.* 280 (2005): 19958–19965.
- [18] I. M. Kulić, H. Schiessel. DNA spools under tension. *Phys. Rev. Lett.* 92. (2004): 228101–1–4.
- [19] For reviews: M. D. Frank-Kamenetskii. Biophysics of the DNA molecule. *Phys. Rep.* 288 (1997): 13–60. T. Schlick. Modeling superhelical DNA – recent analytical and dynamic approaches. *Curr. Opin. Struct. Biol.* 5 (1995): 245–262.
- [20] E. Evans, K. Ritchie. Dynamic strength of molecular adhesion bonds. *Biophys. J.* 72 (1997): 1541–1555. E. Evans. Looking inside molecular bonds at biological interfaces with dynamic force spectroscopy. *Biophys. Chem.* 82 (1999): 83–97.
- [21] H. A. Kramers. Brownian motion in a field of force and the diffusion model of chemical reactions. *Physica (Utrecht)* 7 (1940): 284–304.
- [22] B. Brower-Toland, D. A. Wacker, R. M. Fulbright, J. T. Lis, W. L. Kraus, M. D. Wang. Specific contributions of histone tails and their acetylation to the mechanical stability of nucleosomes. *J. Mol. Biol.* 346 (2005): 135–146.
- [23] J. L. Workman, R. E. Kingston. Alteration of nucleosome structure as a mechanism of transcriptional regulation. *An. Rev. Biochem.* 67 (1998): 545–579.
- [24] G. Li, M. Levitus, C. Bustamante, J. Widom. Rapid spontaneous accessibility of nucleosomal DNA. *Nat. Struct. Mol. Biol.* 12 (2005): 46–53.
- [25] M. Tomschik, H. Zheng, K. van Holde, J. Zlatanova, S. H. Leuba. Fast, long-range, reversible conformational fluctuations in nucleosomes revealed by single-pair fluorescence resonance energy transfer. *Proc. Natl. Acad. Sci. USA* 102 (2005): 3278–3283.
- [26] S. Pennings, G. Meersseman, E. M. Bradbury. Mobility of positioned nucleosomes on 5 S rDNA. *J. Mol. Biol.* 220 (1991): 101–110.
- [27] G. Meersseman, S. Pennings, E. M. Bradbury. Mobile nucleosomes — A general behavior. *EMBO J.* 11 (1992): 2951–2959.
- [28] S. Pennings, G. Meersseman, E. M. Bradbury. Linker histones H1 and H5 prevent the mobility of positioned nucleosomes. *Proc. Natl. Acad. Sci. USA* 91 (1994): 10275–10279.

- [29] A. Flaus, T. J. Richmond. Positioning and stability of nucleosomes on MMTV 3'LTR sequences. *J. Mol. Biol.* 275 (1998): 427–441.
- [30] R. D. Kornberg, Y. Lorch. Twenty-five years of the nucleosome, fundamental particle of the eukaryote chromosome. *Cell*, 98 (1999): 285–294.
- [31] P. B. Becker. Nucleosome sliding: Facts and fiction. *EMBO J.* 21 (2002): 4749–4753.
- [32] A. Flaus, T. Owen-Hughes. Mechanisms for nucleosome mobilization. *Biopolymers* 68 (2003): 563–578.
- [33] H. Schiessel, J. Widom, R. F. Bruinsma, W. M. Gelbart. Polymer reptation and nucleosome repositioning. *Phys. Rev. Lett.* 86 (2001) . 4414–4417; Erratum: *Phys. Rev. Lett.* 88 (2002) 129902-1.
- [34] I. M. Kulić, H. Schiessel. Nucleosome repositioning via loop formation. *Biophys. J.* 84 (2003): 3197–3211.
- [35] I. M. Kulić, H. Schiessel. Chromatin dynamics: nucleosomes go mobile through twist defects. *Phys. Rev. Lett.* 91. (2003): 148103–1-4.
- [36] J. M. Gottesfeld, J. M. Belitsky, C. Melander, P. B. Dervan, K. Luger. Blocking transcription through a nucleosome with synthetic DNA ligands. *J. Mol. Biol.* 321 (2002): 249–263.
- [37] C. Anselmi, G. Bocchinfuso, P. De Santis, M. Savino, A. Scipioni. A theoretical model for the prediction of sequence-dependent nucleosome thermodynamic stability. *Biophys. J.* 79 (2000): 601–613.
- [38] S. Mattei, B. Sampaiole, P. De Santis, M. Savino. Nucleosome organization on *Kluyveromyces lactis* centromeric DNAs. *Biophys. Chem.* 97 (2002): 173–187.
- [39] R. K. Suto, R. S. Edayathumangalam, C. L. White, C. Melander, J. M. Gottesfeld, P. B. Dervan, K. Luger. Crystal structure of nucleosome core particles in complex with minor groove DNA-binding ligands. *J. Mol. Biol.* 326 (2003): 371–380.
- [40] F. Mohammad-Rafiee, I. M. Kulić, H. Schiessel. Theory of nucleosome corkscrew sliding in the presence of synthetic DNA ligands. *J. Mol. Biol.* 344 (2004): 47–58.
- [41] R. S. Edayathumangalam, P. Weyermann, P. B. Dervan, J. M. Gottesfeld, K. Luger. Nucleosomes in solution exist as a mixture of twist-defect states. *J. Mol. Biol.* 345 (2005): 103–114.
- [42] P. T. Lowary, J. Widom. New DNA sequence rules for high affinity binding to histone octamer and sequence-directed nucleosome positioning. *J. Mol. Biol.* 276 (1998): 19–42.
- [43] Y. Lorch, M. Zhang, R. D. Kornberg. Histone octamer transfer by a chromatin-remodeling complex. *Cell* 96 (1999): 389–392.
- [44] G. Längst, P. B. Becker. ISWI induces nucleosome sliding on nicked DNA. *Mol. Cell.* 8 (2001): 1085–1092.
- [45] M. D. Wang, M. J. Schnitzer, H. Yin, R. Landick, J. Gelles, S. M. Block. Force and velocity measured for single molecules of RNA polymerase. *Science* 282 (1998): 902–907.
- [46] F. Jülicher, R. Bruinsma. Motion of RNA polymerase along DNA: A stochastic model. *Biophys. J.* 74 (1998): 1169–1185.
- [47] H.-Y. Wang, T. Elston, A. Mogilner, G. Oster. Force generation in RNA polymerase. *Biophys. J.* 74 (1998): 1186–1202.
- [48] V. M. Studitsky, D. J. Clark, G. Felsenfeld. A histone octamer can step around a transcribing RNA polymerase without leaving the template. *Cell* 76 (1994): 371–382.

- [49] V. M. Studitsky, D. J. Clark, G. Felsenfeld. Overcoming a nucleosomal barrier to transcription. *Cell* 83 (1995): 19–27.
- [50] V. M. Studitsky, G. A. Kassavetis, E. P. Geiduschek, G. Felsenfeld. Mechanism of transcription through the nucleosome by eukaryotic RNA polymerase. *Science* 278 (1997): 1960–1963.
- [51] J. Bednar, V. M. Studitsky, S. A. Gregoryev, G. Felsenfeld, C. L. Woodcock. The nature of the nucleosomal barrier to transcription: Direct observation of paused intermediates by electron cryomicroscopy. *Mol. Cell* 4 (1999): 377–386.
- [52] R. U. Protacio, J. Widom. Nucleosome transcription studied in a real-time synchronous system: test of the lexosome model and direct measurement of effects due to histone octamer. *J. Mol. Biol.* 256 (1996): 458–472.
- [53] B. ten Heggeler-Bodier, C. Schild-Poulter, S. Chapel, W. Wahli. Fate of linear and supercoiled multinucleosomal templates during transcription. *EMBO J.* 14 (1995): 2561–2569.
- [54] B. ten Heggeler-Bodier, S. Muller, M. Monestier, W. Wahli. An immuno-electron microscopical analysis of transcribing multinucleosomal templates: What happens to the histones? *J. Mol. Biol.* 299 (2000): 853–858.
- [55] B. Dorigo, T. Schalch, A. Kulangara, S. Duda, R. R. Schroeder, T. J. Richmond. Nucleosome arrays reveal the two-start organization of the chromatin fiber. *Science* 306 (2004): 1571–1573.
- [56] T. Odijk, A. C. Houwaart. Theory of excluded volume effect of a polyelectrolyte in a 1-1 electrolyte solution. *J. Polym. Sci.* B16, (1978): 627–639.
- [57] C. Münkler, J. Langowski. Chromosome structure predicted by a polymer model. *Phys. Rev. E* 57 (1998): 5888–5896.
- [58] G. Wedemann, J. Langowski. Computer simulation of the 30-nanometer chromatin fiber. *Biophys. J.* 82 (2002): 2847–2859.
- [59] B. Mergell, R. Everaers, H. Schiessel. Nucleosome interactions in chromatin: fiber stiffening and hairpin formation. *Phys. Rev. E* 70. (2004): 011915–1-9.
- [60] S. Mangenot, A. Leforestier, P. Vachette, D. Durand, F. Livolant. Salt-induced conformation and interaction changes of nucleosome core particles. *Biophys. J.* 82 (2002): 345–356.
- [61] S. Mangenot, E. Raspaud, C. Tribet, L. Belloni, F. Livolant. Interactions between isolated nucleosome core particles: A tail-bridging effect? *Eur. Phys. J. E* 7 (2002): 221–231.
- [62] A. Bertin, A. Leforestier, D. Durand, F. Livolant. Role of histone tails in the conformation and interactions of nucleosome core particles. *Biochemistry* 43 (2004): 4773–4780.
- [63] H. Boroudjerdi, R. R. Netz. Interactions between polyelectrolyte-macroion complexes. *Europhys. Lett.* 64 (2003): 413–419.
- [64] H. Boroudjerdi, R. R. Netz. Strongly coupled polyelectrolyte-macroion complexes. *J. Phys. Condens. Matter* 17 (2005): S1137–S1151.
- [65] I. Rouzina, V. A. Bloomfield. Macroion attraction due to electrostatic correlation between screening counterions. 1. Mobile surface adsorbed ions and diffuse ion cloud. *J. Phys. Chem.* 100 (1996): 9977–9989.
- [66] E. Allahyarov, H. Löwen, J. P. Hansen, A. A. Louis. Nonmonotonic variation with salt concentration of the second virial coefficient in protein solutions. *Phys. Rev. E* 67. (2003): 051404–1-13.

- [67] R. Podgornik. Two-body polyelectrolyte-mediated bridging interactions. *J. Chem. Phys.* 118 (2003): 11286–11296.
- [68] T. Åkesson, C. Woodward, B. Jönsson. Electric double layer forces in the presence of polyelectrolytes. *J. Chem. Phys.* 91 (1989): 2461–2469.
- [69] S. J. Miklavic, C. E. Woodward, B. Jönsson, T. Åkesson. Interaction of charged surfaces with grafted polyelectrolytes: A Poisson-Boltzmann and Monte Carlo study. *Macromolecules* 23 (1990): 4149–4157.
- [70] M. K. Granfeldt, B. Jönsson, C. E. Woodward. A Monte Carlo simulation study of the interaction between charged colloids carrying adsorbed polyelectrolytes. *J. Phys. Chem.* 95 (1991): 4819–4826.
- [71] R. Podgornik, T. Åkesson, B. Jönsson. Colloidal interactions mediated via polyelectrolytes. *J. Chem. Phys.* 102 (1995): 9423–9434.
- [72] F. Mühlbacher, C. Holm, H. Schiessel. Controlled DNA compaction within chromatin: The tail-bridging effect. *Europhys. Lett.* 73 (2006): 135–141.
- [73] D. Frenkel, B. Smit. *Understanding Molecular Simulation*. 2nd ed. Academic Press, San Diego, 2002.
- [74] K. Kremer, G. S. Grest. Dynamics of entangled linear polymer melts. *J. Chem. Phys.* 92 (1990): 5057–5086.
- [75] D. A. McQuarrie. *Statistical Mechanics*. Harper-Collins, New York, 1976.
- [76] S. Alexander, P. M. Chaikin, P. Grant, G. J. Morales, P. Pincus, D. Hone. Charge renormalization, osmotic pressure, and bulk modulus of colloidal crystals—Theory. *J. Chem. Phys.* 80 (1984): 5776–5781.
- [77] J. Sun, Q. Zhang, T. Schlick. Electrostatic mechanism of nucleosomal array folding revealed by computer simulation. *Proc. Natl. Acad. Sci. USA* 102 (2005): 8180–8185.
- [78] P. J. Horn, C. L. Peterson. Chromatin higher order folding: wrapping up transcription. *Science* 297 (2002): 1824–1827.
- [79] C. Tse, T. Sera, A. P. Wolffe, J. C. Hansen. Disruption of higher-order folding by core histone acetylation dramatically enhances transcription of nucleosomal arrays by RNA polymerase III. *Mol. Cell. Biol.* 18 (1998): 4629–4638.
- [80] M. F. Dion, S. J. Altschuler, L. F. Wu, O. J. Rando. Genomic characterization reveals a simple histone H4 acetylation code. *Proc. Natl. Acad. Sci. USA* 102 (2005): 5501–5506.
- [81] M. L. Kireeva, W. Walter, V. Tchernajenko, V. Bondarenko, M. Kashlev, V. M. Studitsky. Nucleosome remodelling induced by RNA polymerase II: Loss of the H2A/H2B dimer during transcription. *Mol. Cell* 9 (2002): 541–552.
- [82] A. Flaus, T. Owen-Hughes. Mechanisms for ATP-dependent chromatin remodelling: Farewell to the tuna-can octamer? *Curr. Opin. Genet. Dev.* 14 (2004): 165–173.